R-99-08

On the simulation of variable density flow at SFR, Sweden

Martin Stigsson, Sven Follin, Johan Andersson
Golder Grundteknik KB

December 1998

Svensk Kärnbränslehantering AB
Swedish Nuclear Fuel
and Waste Management Co
Box 5864
SE-102 40 Stockholm Sweden
Tel 08-459 84 00
+46 8 459 84 00
Fax 08-661 57 19
+46 8 661 57 19

ISSN 1402-3091
SKB Rapport R-99-08

On the simulation of variable density flow at SFR, Sweden

Martin Stigsson, Sven Follin, Johan Andersson
Golder Grundteknik KB

December 1998

Summary

The main objective of this work is to investigate if variable-density groundwater flow during a continuous shore level displacement at SFR can be treated as uniform-density flow where salinity is modelled as a tracer. If the difference between modelling the groundwater as a variable-density or uniform-density is small, or if small changes in other parameters with high uncertainty largely impact the result, then it is likely that a freshwater code may give equitable results of the groundwater conditions at SFR.

The Finite Element code SUTRA (Voss, 1984) is used for the 2-D studies. In all 52 cases are studied and the results from the most interesting and relevant cases are presented. Most of the cases are more or less generic to be able to study one parameter at the time. The changed parameters are:

- Permeability
- Porosity
- Change in long term evolution of the salinity in the sea water
- Presence of vertical and/or horizontal structures

The last presented case is a case where data from Axelsson and Hansen (1997) has been used to make a model that is as real as possible.

The most important conclusions are:

- The porosity has a large impact on the results since higher porosity means that the transport time is longer and that more saline water has to be flushed out.

- As the model becomes more complex (i.e., incorporating parameter heterogeneity, structures, etc.) the spatial differences in salinity and the difference in flow through the SFR, between variable-density and uniform-density flow, becomes less significant.

- Differences between modelling groundwater as a variable-density flow or a uniform-density flow with salt as a tracer at the SFR is negligible.

Table of contents

1 INTRODUCTION

The main objective of this work is to investigate if variable-density groundwater flow during a continuous shore level displacement at the SFR can be treated as uniform-density flow where salinity is modelled as a tracer. Secondly, the work also addresses sensitivities in the various model parameters such as permeability, porosity, structures and salinity in the seawater.

The background for doing the simulations in this work is presented in SKB (1998) where it is suggested that a generic model is developed to investigate the density effects. Voss and Andersson (1993) demonstrated that the transient effects induced by shore level displacement have a more important control of the groundwater velocity field than the effects of density variations. Furthermore, given the quite shallow location of the SFR (around 50 m below the rock surface) the density effects on the deep groundwater circulation can be judged to be relatively unimportant. Numerical calculations are used to substantiate these suggestions.

If the spatial difference in salinity and the difference in flow is small between modelling the groundwater as a variable-density or uniform-density, or if small changes in other parameters with high uncertainty largely impact the result, then it is likely that a freshwater code may give equitable results of the groundwater conditions at SFR.

2 HYDROGEOLOGIC SETTING

2.1 Topography

North-eastern Uppland is characterised by an undulating landscape with no major hills or valleys. Rivers and peat bogs in the area are situated in the small depressions indicating that the groundwater level is almost the same as the ground level. The landscape declines weakly towards the Baltic with a general trend in the slope of 2-3‰ towards the north-east. This trend continues under the sea level of the Baltic Sea (Axelsson et al., 1983).

The area around Forsmark and SFR is shown in Figure 2-1. Section A-B in Figure 2-1 is approximately perpendicular to the altitude contours of the area. The surface of the ground along the section A-B is plotted in Figure 2-2.

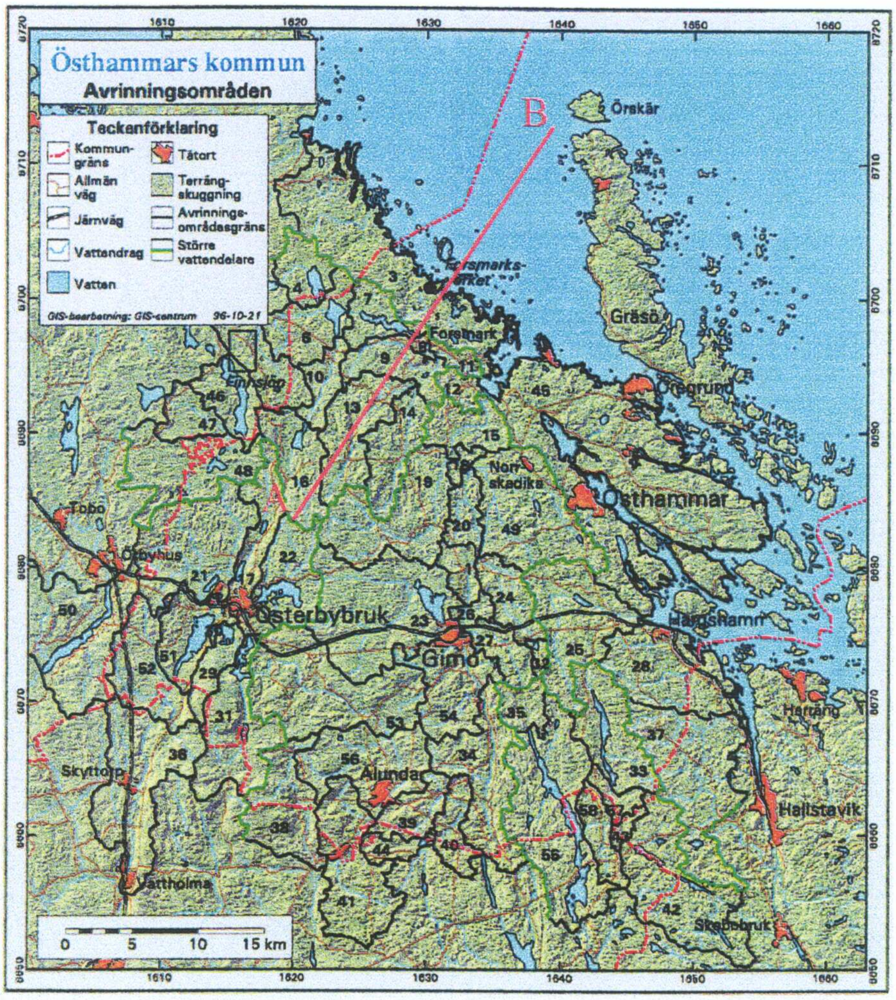

Figure 2-1. Map over the municipality of Östhammar. Major (green) and minor (black) watersheds are shown. The topography along the red line A-B is shown in Figure 2-2.

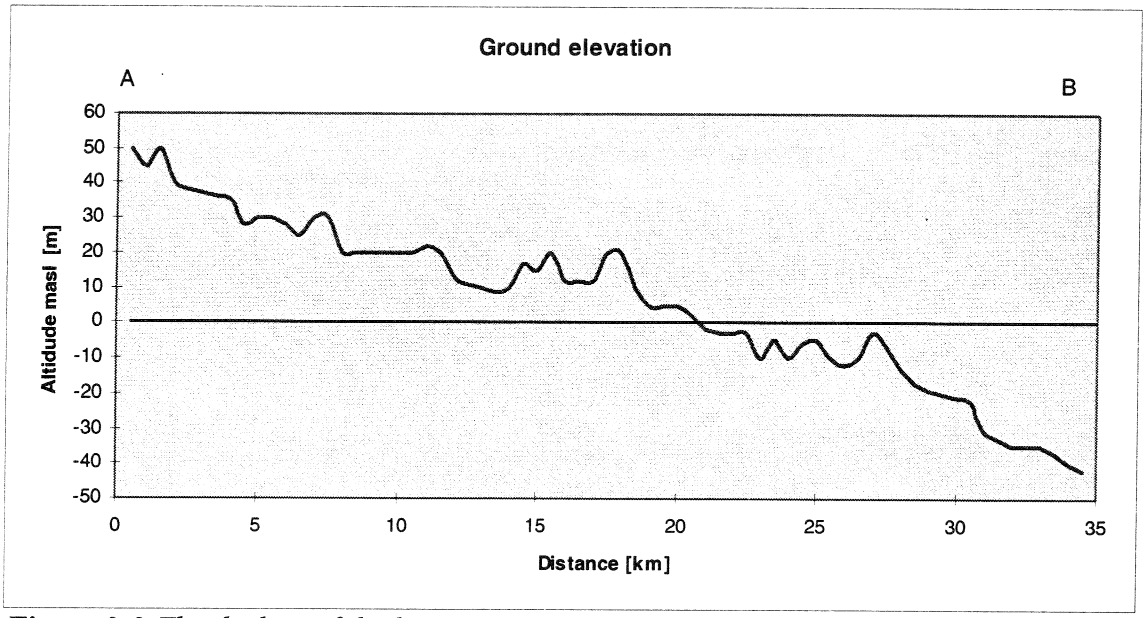

Figure 2-2. The decline of the line A-B in Figure 2-1.

2.2 Bedrock

The hydrogeologic model used in the latest assessment at the SFR (SKB, 1993) are presented by Carlsson et al. (1986). This model has been reassessed by Axelsson and Hansen (1997).

According to Axelsson (1986) the bedrock of Forsmark mainly consists of gneiss granite and gneiss with dikes and small massifs of greenstones and pegmatite. The gneiss granite and the gneiss are fine to middle grained.

The bedrock is covered by quaternary deposits, which mainly consists of sandy till. The thickness of the layer is normally 4-5 m and has a levelling effect on the surface. Areas of thin soil coverage or minor rock outcrops are frequent in the region around Forsmark (Carlsson and Olsson, 1981).

The deposits under the Baltic consist generally of till covered by fine sediments such as clay. According to VBB (1973) the clay layer is about 2-4 m and the underlying till layer is 3-6 m. Also at the sea bottom the soil layers have a levelling effect on the topography. The clay layers are impermeable or semi-impermeable which implies that they may leak freshwater from the sea bottom into the Baltic.

To describe the relationship of hydraulic conductivity with depth Carlsson et al. (1986) assumed a power-law expression of the form

$$K = A \cdot z^{-b} \tag{2-1}$$

where

z = Depth [m]
A = Coefficient that states the value of the regression model at the depth of 1 m [m]
b = Coefficient describing the depth decrease [-]

Follin et al. (1996) compared hydraulic information from shallow groundwater wells from the Well Archive at the Swedish geological survey with information from the deeper boreholes in Finnsjön Study Area and SFR. The authors concluded that there are great differences in the perceived depth dependence between shallow and deep data records.

Axelsson and Hansen (1997) noted that the depth-decrease relationships are highly questionable. By reinterpreting hydraulic data from some SKB study areas Walker et al. (1997) find that there is no statistical support for a hydraulic conductivity decrease below a certain depth. Reinterpretation of the SFR hydraulic data would possibly give the same result.

The depth-dependent hydraulic conductivity of the different data sets is plotted in Figure 2-3.

In the neighbourhood of SFR there are three major zones, two vertical and one subhorizontal. There are also several minor zones in different directions.

The most dominant zone is the so called Singö zone. The width of the Singö zone is about 200 m, with a core of about 50 m with a high frequency of open fractures (Axelsson, 1986). The core is assumed to have a hydraulic conductivity of $5 \cdot 10^{-7}$ m/s (SKB, 1993).

West of the Singö zone is the other vertical zone, the Forsmark zone. According to Axelsson (1986) this zone is supposed to have the same properties as the Singö zone.

The subhorizontal zone is known as the H2 zone. The zone has a WSW strike and the dip is 20° to the South. This zone is probably extended beyond the Singö zone towards SW and reaches the sea bottom at the NE (Axelsson and Hansen 1997). The zone is assumed to have a width of 10 m and a hydraulic conductivity of $1 \cdot 10^{-6}$ m/s (SKB, 1993).

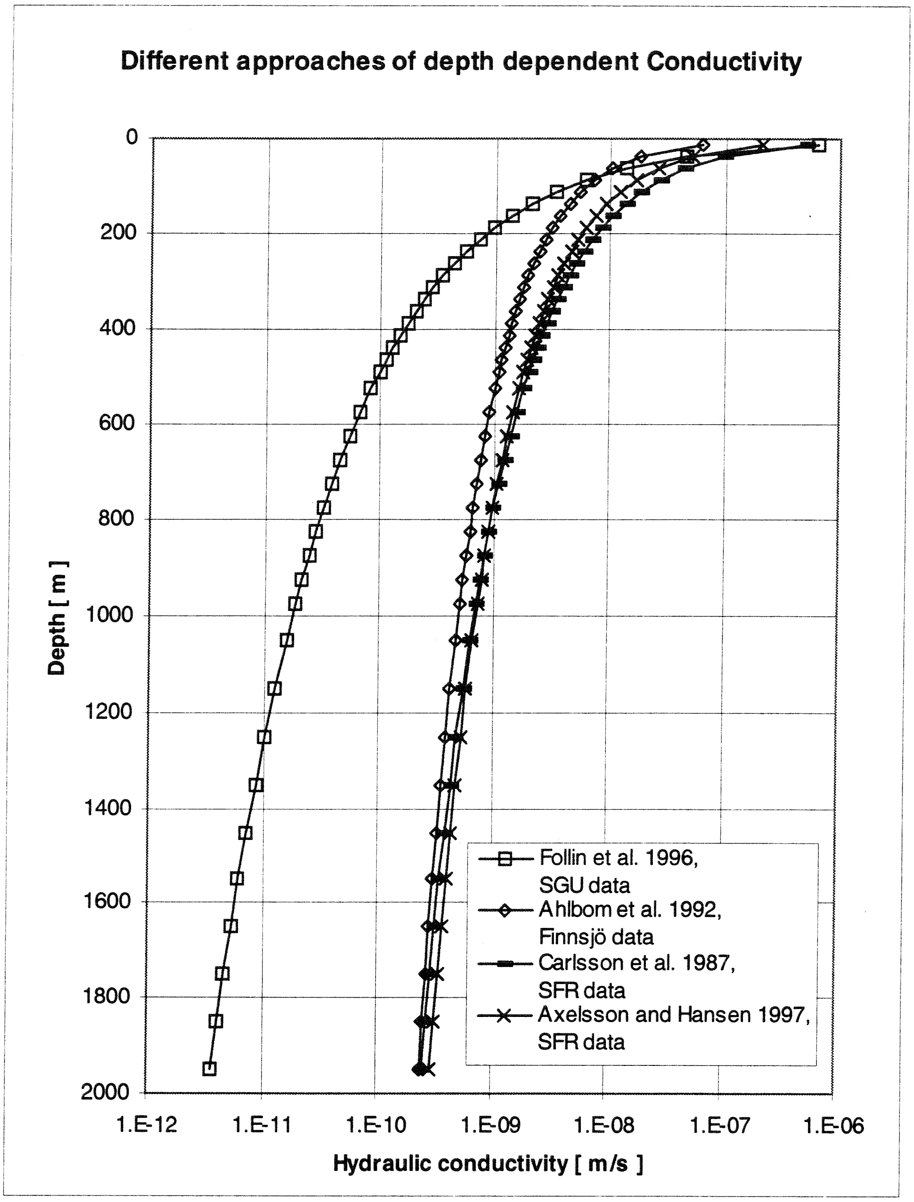

Figure 2-3. *Comparison between different data sets.*

2.3 Hydrologic Evolution

2.3.1 Shore level displacement

The largest extension of the latest glacial period occurred about 20 000 years ago. Large amounts of water were tied to the ice mass, which had a maximum thickness of about 3 km. This resulted in the water levels of the oceans being about 120 m below their present levels. Under the pressure from the ice the earth crust was 800 m below the level of today (Follin et al., 1996).

When the ice began to melt both the land and the water level increased. The interplay between land, ice and the water has resulted in different water types in the Baltic Sea as well as in the Baltic shield rock. In some periods the Baltic Sea was a freshwater lake while in others it was a saline sea.

The difference between ground level changes and the sea level change is called shore level displacement. A mathematical model of these phenomena is presented by Påsse (1996). Figure 2-4 shows the model for Forsmark from 10 000 years BP, before present, to 5 000 years AP, after present, where present is taken as 1950.

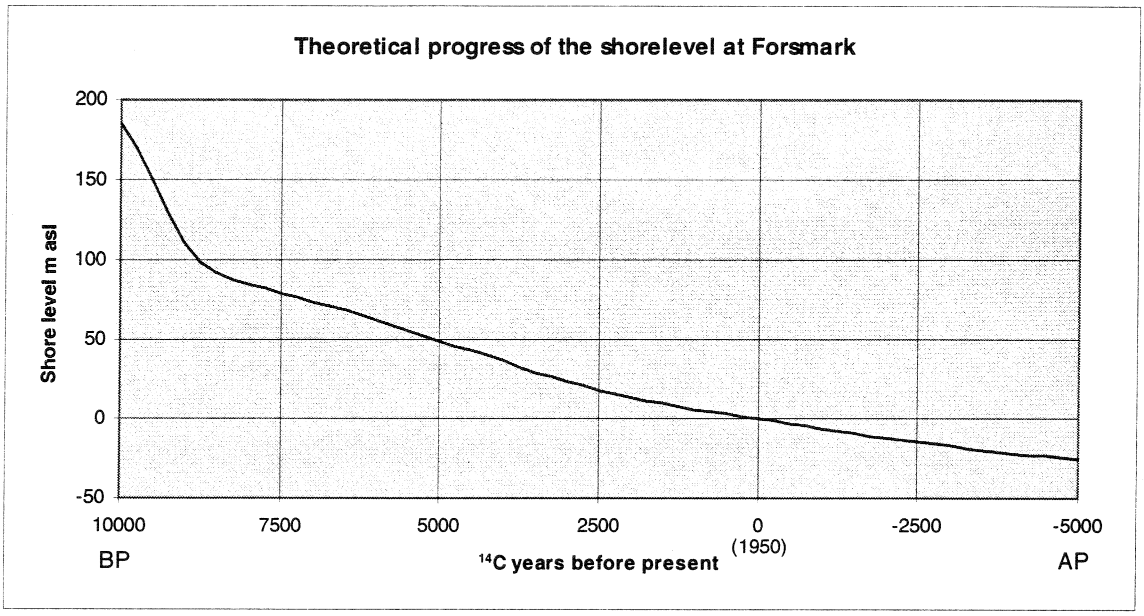

Figure 2-4. *The progress of the shore level for the last 10 000 years and prediction for 5 000 years into the future, Påsse (1996)*

2.3.2 Evolution of salinity in the Baltic

The salinity of the Baltic Sea during the last 10 000 years has been investigated by Westman (1997). The Baltic Ice Lake, before 9 300 BP, was a lake that either had none or only very low salinity (0-2‰). During existence of the Yoldia Sea, 9 300-8 600 BP, there was a connection to the North Sea through the Närke Sound. During this period, saltwater intruded for about 100 years. The next phase in the evolution, 8 600 BP-7 200 BP, the Ancylus Lake contained non-saline water.

The Litorina Sea, 7 200 BP-0 BP, is divided into three sub-phases, none of which is well defined neither with time nor with salinity. During the first 1 000 years the salinity increased to 12-15‰. Thereafter the salinity was constant for about 2 000 years. The high salinity may be explained by the fact that during this time period the water level in Öresund and The Belts was the highest ever. At about 5 000 BP the salinity began to decrease, and 2 000-1 500 BP a second decrease in the salinity took place, during which the concentration of salt became the same as today.

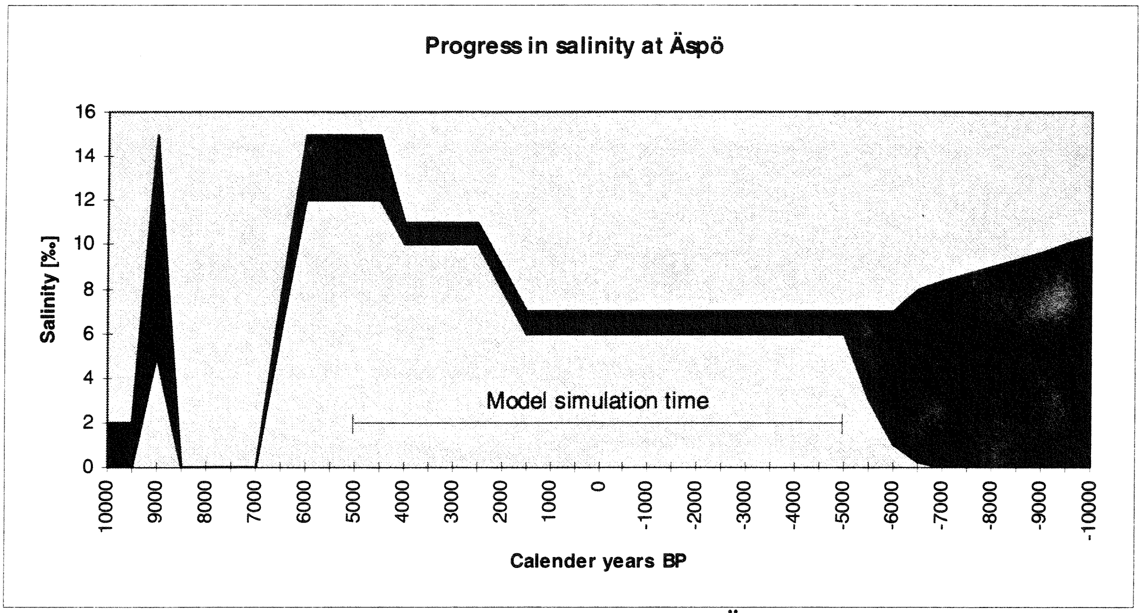

Figure 2-5. *The evolution of the salinity of the Baltic at Äspö from 10 000 years BP and prediction of the future progress.*

Today the salinity of the surface water outside Forsmark is about 5‰ according to Marine Ecosystem Modeling Group (1996). Depending on which scenario that occurs the salinity will increase or decrease in the future. According to Kautsky (1998) it will be constant for the next 5 000 years at Äspö. SFR is located 400 km to the North and the progress in salinity will not fully coincides with the progress at Äspö. The bottom topography of the Baltic Sea shows that SFR is situated north of a topographic threshold, c.f. Figure 2-6. This will probably make the seawater in the vicinity of SFR less saline in the future due to the difficulty for the heavy saline water to pass the topographic threshold.

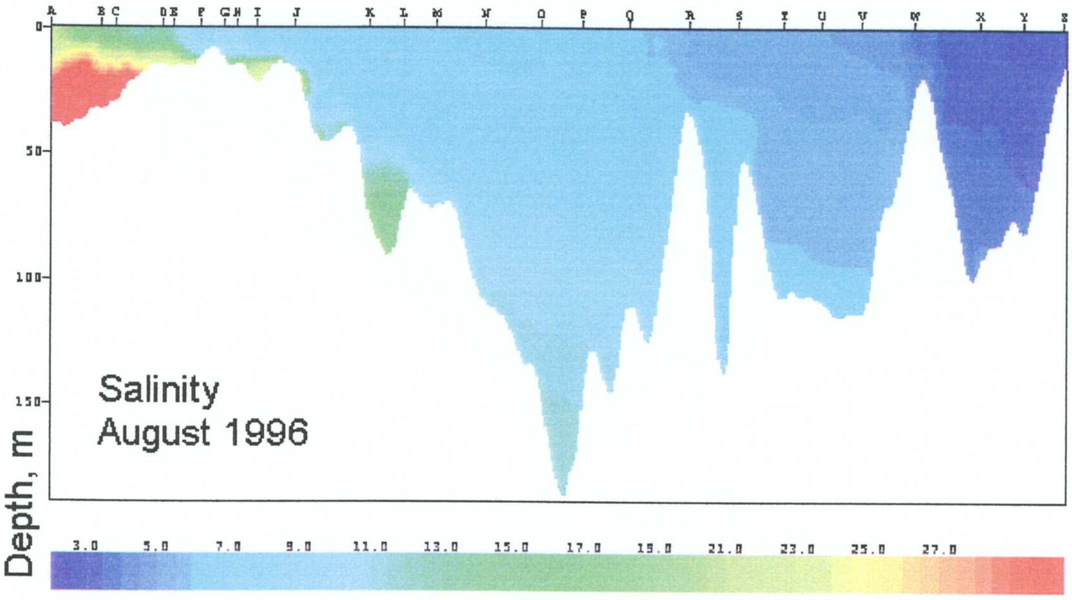

Salinity in PSU (Practical Salinity Units) which is almost the same as g salt per kg seawater.

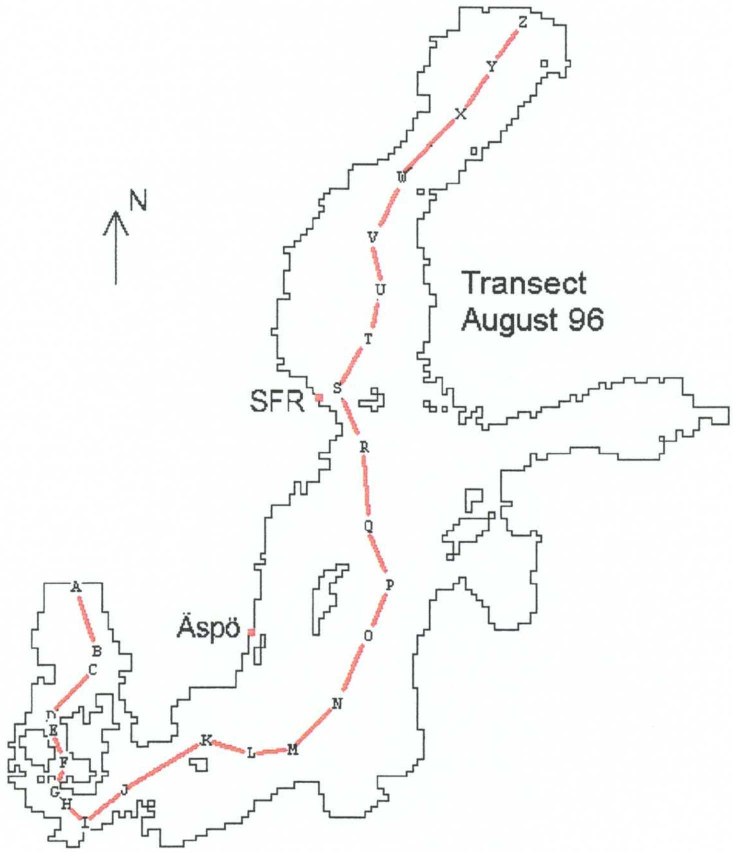

Figure 2-6. *A salinity profile for the Baltic Sea in August 1996, according to Marine Ecosystem Modeling Group (1996). In the upper figure is also the bottom topography shown along the profile. The salinity at point "s", outside SFR, is estimated to 5‰.*

3 Hydrogeologic model

The purpose of the hydrogeologic modelling is to investigate if saline water can be modelled as a uniform-density flow where salinity is modelled as a tracer instead of a variable-density flow. This can be done by investigating if the groundwater flow and the spatial distribution of the salinity are more sensitive to the difference in water density than to the sensitivities in permeability, porosity, location of zones and change in the long-term evolution of the sea water salinity.

3.1 Governing equations

In order to meet the outlined purpose, a 2-D porous medium approach has been used. Because of the large scale of the problem, a porous medium approach is a fair assumption. To ensure that the 2-D model is representative it is important that the modelled cross-section is parallel to the groundwater flow paths. This will almost be fulfilled if the section is perpendicular to the altitude contours of the bedrock and surface provided that the hydraulic anisotropy is of minor importance.

Since the problem contains both fresh and saline waters it is necessary to consider both pressure-driven flow and density-driven flow. The mechanisms of pressure and density driving forces for saturated flow through a porous medium may be expressed by the following general form of Darcy's law

$$\overline{v} = \frac{\overline{\overline{k}}}{n\mu} \cdot \left(\overline{\nabla} p - \rho \overline{g}\right) \qquad (3\text{-}1)$$

where

$\overline{v}$ = Average fluid velocity [m/s]

$\overline{\overline{k}}$ = Permeability [m^2]

n = Porosity [-]

μ = Viscosity [Ns/m^2]

p = Pressure [Pa]

ρ = Density [kg/m^3]

g = Constant of gravity [m/s^2]

The fluid mass balance equation may be written as the sum of pure water and pure solute mass balances

$$\frac{\partial(n\rho)}{\partial t} = -\overline{\nabla} \cdot \left(n\rho\overline{v}\right) + Q + T \qquad (3\text{-}2)$$

where

n = Porosity [-]
ρ = Density [kg/m^3]
t = Time [s]
$\overline{v}$ = Velocity [m/s]
Q = Fluid mass source [kg/(m^3·s)]
T = Solute mass source [kg/(m^3·s)]

The pure solute mass source term, T, may account for external additions of pure solute mass not associated with a fluid source. In most cases this contribution is small compared to the total pure water mass contributed by the fluid sources, Q. Therefor the solute mass source, T, is neglected. The equation for solving the transport of the salt is described by

$$\frac{\partial(n\rho C)}{\partial t} = -\overline{\nabla} \cdot \left(n\rho\overline{v}C\right) + \overline{\nabla} \cdot \left(n\rho(D_m \overline{\overline{I}} + \overline{\overline{D}}) \cdot \overline{\nabla}C \right) + Q \cdot C^* \qquad (3\text{-}3)$$

where

n = Porosity [-]
ρ = Density [kg/m^3]
C = Concentration of the fluid as mass fraction [kg/kg]
t = Time [s]
$\overline{v}$ = Velocity [m/s]
D_m = Molecular diffusivity of solute [m^2/s]
$\overline{\overline{I}}$ = Unity tensor [-]
$\overline{\overline{D}}$ = Dispersion tensor [m^2/s]
Q = Fluid mass source [kg/(m^3·s)]
C^* = Solute concentration of fluid source as mass fraction [kg/kg]

The relationship between salinity and density is assumed to be a linear function described by

$$\rho = \rho_{fresh} + A \cdot C \qquad (3\text{-}4)$$

where

ρ = Density of the saline water [kg/m^3]
ρ_{fresh} = Density of the fresh water, base concentration, assumed to 998.2 [kg/m^3]
A = A factor that is valid in a small range of salinity near the base concentration, assumed to be 700, according to Voss (1984) [kg/m^3]
C = Concentration of salt in the saline water [kg/kg]

3.2 Simulated time

The time when the simulation starts is 5 000 years BP (before present) where present is taken as 1950, the simulation then proceeds for 10 000 years, i.e. the simulation ends at 5 000 years AP (after present). The start time for the simulations is chosen due to that the salinity has been stable during the previous 1 000 years in the Baltic Sea, and the fact that the studied section has been under water since the last glacial period. The end of the simulation time is when the salinity of the water in the Baltic Sea is assumed to start to increase or decrease significantly again, c.f. Figure 2-5.

3.3 Boundary conditions

The selection of proper boundary conditions is crucial for the modelling results. When the flow across a boundary is known, a specified flow condition can be used. A special case of the specified flow is the no-flow boundary that can be used if the boundary is situated at a water divide, or if it is placed far away from the studied target area. Far away is subjective and is interpreted to imply a location where the impact on the groundwater flow in the area of interest is negligible. If the concentration of the fluid at the boundary is known then it is possible to use a specified concentration condition.

3.3.1 Vertical inland boundary

The location of this boundary is chosen so that it coincides with a major groundwater divide, see Figure 2-1 and Figure 3-1, which implies that a no-flow boundary will be a good approximation. Secondly, the boundary roughly coincides with the position of the shore level at the simulation start 5 000 years BP, see Figure 2-4.

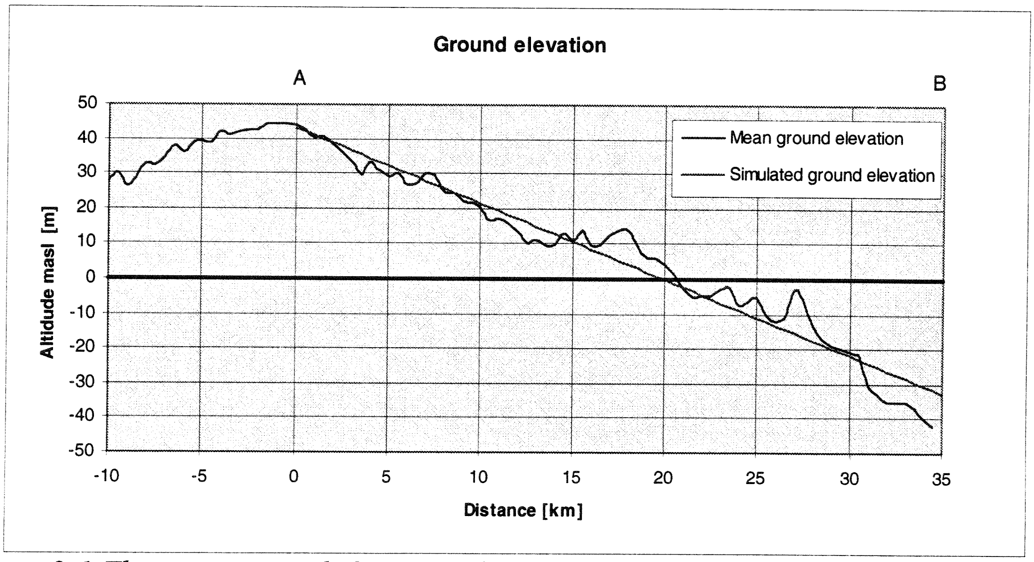

Figure 3-1. *The mean ground elevation along the section from south-west to north-east and the approximated ground surface of the upper boundary of the simulations. The slope is set to 2.2‰.*

3.3.2 Bottom boundary

The depth of the model domain is chosen to be 2 km. This depth has been shown to be sufficient in similar studies, see for example Voss and Andersson (1993) and Follin (1995). The small velocities of the groundwater flow at large depths suggest that a no-flow boundary at 2 km depth will probably fulfil the purposes of the modelling.

3.3.3 Vertical off shore boundary

This boundary is the most difficult boundary to specify since the topography continues to decline toward north. However, according to Voss and Andersson (1993) it may be possible to use a no-flow boundary if the boundary is sufficiently far away from the target area.

3.3.4 Top boundary

To reduce the effect of local heights and depressions which may cause water to flow perpendicular to the modelled cross section, the mean elevations of a 5 km wide strip is taken as a representative value of the elevation of the cross section. At the sea bottom there is lack of elevation data and the topography from Axelsson (1986) is taken as a representative value for the section.

The top boundary is characterised by a transient specified pressure and a transient specified concentration of salinity. In short, the pressure changes are set to mimic the shore level displacement described in Figure 2-4. Likewise the pressure at the sea floor simulates the ambient depth and salinity of the seawater. When the top boundary becomes land, instead of sea bottom, the pressure is atmospheric and the concentration of salt is zero.

The progress of the salinity at the top of the model is approximated by a linear decrease instead of the stepwise decrease as is shown in Figure 2-5. The first decrease is between 5 000 years BP to 0 years BP where the salinity decreases from 12 or 15‰ to 5‰. The next step is between 0 BP and 5 000 years AP. In this step the salinity is either assumed constant at 5‰, or assumed to decreases linearly to 2‰.

The topography of the section does not vary very much and is approximated by a straight line, c.f. Figure 3-1. Due to the large scale and the small inclination of the ground surface the groundwater table is assumed to be the same as the ground surface and the access of rain water, i.e. infiltration, is unlimited.

The impermeable layers at the sea bottom mentioned in Axelsson (1986) are not taken into account. This is due to the fact that the layer is not continuous, instead, it is thick in the depressions and there is no layer at the heights of the bottom topography.

3.4 Initial conditions

At 5 000 years BP the shore level was at 47 meters above sea level, masl, according to Figure 2-4, while the highest elevation of the section is at 43 masl. Figure 2-4 also shows that the section has been under the sea level for at least 5 000 years.

The Baltic Sea had a constant salinity of 12-15‰ between 6 000 BP and 4 500 BP. Since saline water is heavier than fresh water, it is much faster to replace the freshwater in the bedrock with saline water, than the other way around. Under this basis, the whole section is filled with saline ground water at the beginning of the simulation. The initial pressure represents the hydrostatic conditions for the initial concentration distribution.

3.5 Numerical solution

To get a high accuracy and still have a model that is as small as possible, the finite-element mesh is built with a fine grid in the upper region and in the region where structures are modelled. In the bottom of the model, where there is little flow, a coarse grid is used, see Figure 3-2. The mesh is more detailed in the middle of the studied area, to be able to study effects of structures.

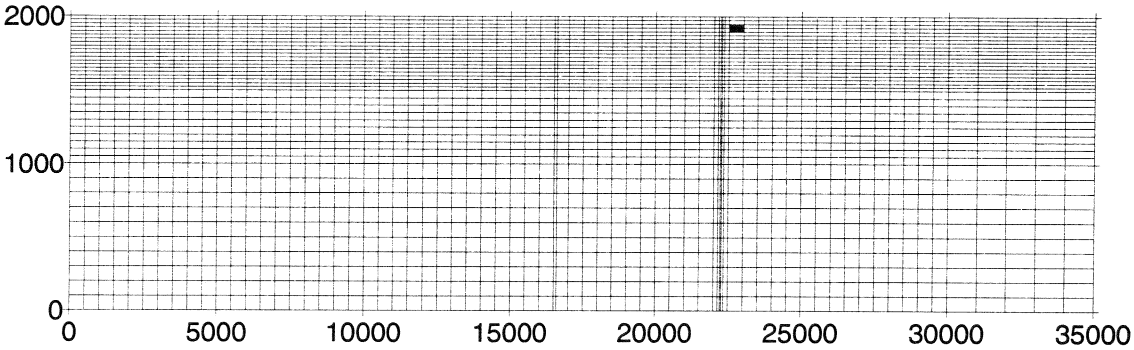

Figure 3-2. *The FE mesh that is used for the simulations. The tick-mark 0 on the horizontal axis corresponds to point A in Figure 2-1 and the tick-mark 35 000 corresponds to point B. On the vertical axis the tick-mark 2000 corresponds to ground level. Observe that the scale on the vertical axis is 5 times the horizontal. The filled elements correspond to the SFR.*

Equations 3-1 to 3-4 together with boundary and initial conditions are solved for the mesh in Figure 3-2 by the finite element code SUTRA (Voss, 1984).

4 Results

Simulation results are plotted at 0 years BP, at 1 000 years AP and at 5 000 years AP. The positions of the shorelines are at these times at 19 600 m, 22 200 m and 30 000 m respectively. As can be seen in Figure 3-2, the SFR is situated at approximately 22 700 m, which means that the hydrogeological conditions of the area where SFR is located will undergo a transition from being located in a discharge (outflow) area to a recharge (infiltration) area. Since the top boundary is approximated by a plane instead of the measured topography, there will be some differences of where the shoreline is situated in the model and in reality at the same time.

4.1 Studied cases

This study comprises 52 simulations with different assumptions regarding rock permeability, porosity, structures and progress of the sea water salinity. Only the most interesting results will be shown.

Table 4-1. Characterisation of the studied cases

Case	Permeability [m^2]	porosity [‰]	Salinity in sea water[1] [‰]	Structures	Comments
Reference	$7 \cdot 10^{-16}$	2	12-5-2	none	
Progress in salinity	$7 \cdot 10^{-16}$	2	15-5-2 12-5-5	none	
High permeability in surface layer	$7 \cdot 10^{-14}$ $7 \cdot 10^{-16}$	2	15-5-5	none	The upper 200 m have the higher value
Correlated porosity to hydraulic conductivity	$7 \cdot 10^{-14}$ $7 \cdot 10^{-16}$	20 2	15-5-5	none	The upper 200 m have the higher value
Highly permeable vertical structures	$7 \cdot 10^{-14}$ $7 \cdot 10^{-16}$	2	15-5-5	2 vertical	The zones have the higher value
Low permeability vertical structures	$7 \cdot 10^{-18}$ $7 \cdot 10^{-16}$	2	15-5-5	2 vertical	The zones have the lower value
Horizontal and vertical structures	$7 \cdot 10^{-14}$ $7 \cdot 10^{-16}$	2	15-5-5	2 vertical and 1 horizontal	The zones have the higher value
Best estimate	depth and structure dependent	2	12-5-5	2 vertical and 1 sub-horizontal	

[1]The figures correspond to the salinity at 5 000 years BP, at 0 years BP and at 5 000 years AP respectively.

Based on the studies by Follin (1995) and Voss and Andersson (1993) the longitudinal dispersivity is set to 200 m and the transverse to 10 m for all simulations. The molecular diffusivity is $5 \cdot 10^{-10}$ m^2/s.

4.2 Reference case

The reference case in this study is a homogeneous cross section of constant permeability $7 \cdot 10^{-16}$ m^2 which corresponds to a fresh water hydraulic conductivity of $5 \cdot 10^{-9}$ m/s. The effective porosity is set to 2‰ throughout the modelled domain. The progress of salinity in the sea water is described by an initial value of 12‰ at the time 5 000 years BP, then the salinity decreases linearly to 5‰ at present and decreases to 2‰ at 5 000 years AP.

4.2.1 Salinity in the modelled profile

The results from the simulations from the reference case are shown in Figure 4-1, where the density varies with salinity, and Figure 4-2 where the density is constant and the salinity is treated as a tracer.

Due to the low hydraulic conductivity the transition zone between saline and fresh groundwater is not at the same place as the shoreline. Two differences in the location of the transition zone can be observed when the simulations in Figure 4-1 and Figure 4-2 are compared. The first is that the fresh water will not flush as deep if variable-density is taken into account. The second observation is that the transition zone will be closer to the shoreline if the variable-density is taken into account. The reason for this is that fresh water will float on top of the saline water when variable-density is assumed.

From these observations, it can be concluded that there are only small spatial differences in salinity between the two approaches. If the permeability had been higher than $7 \cdot 10^{-16}$ m^2 then the spatial differences in salinity would have been even smaller especially at the upper most part of the model domain.

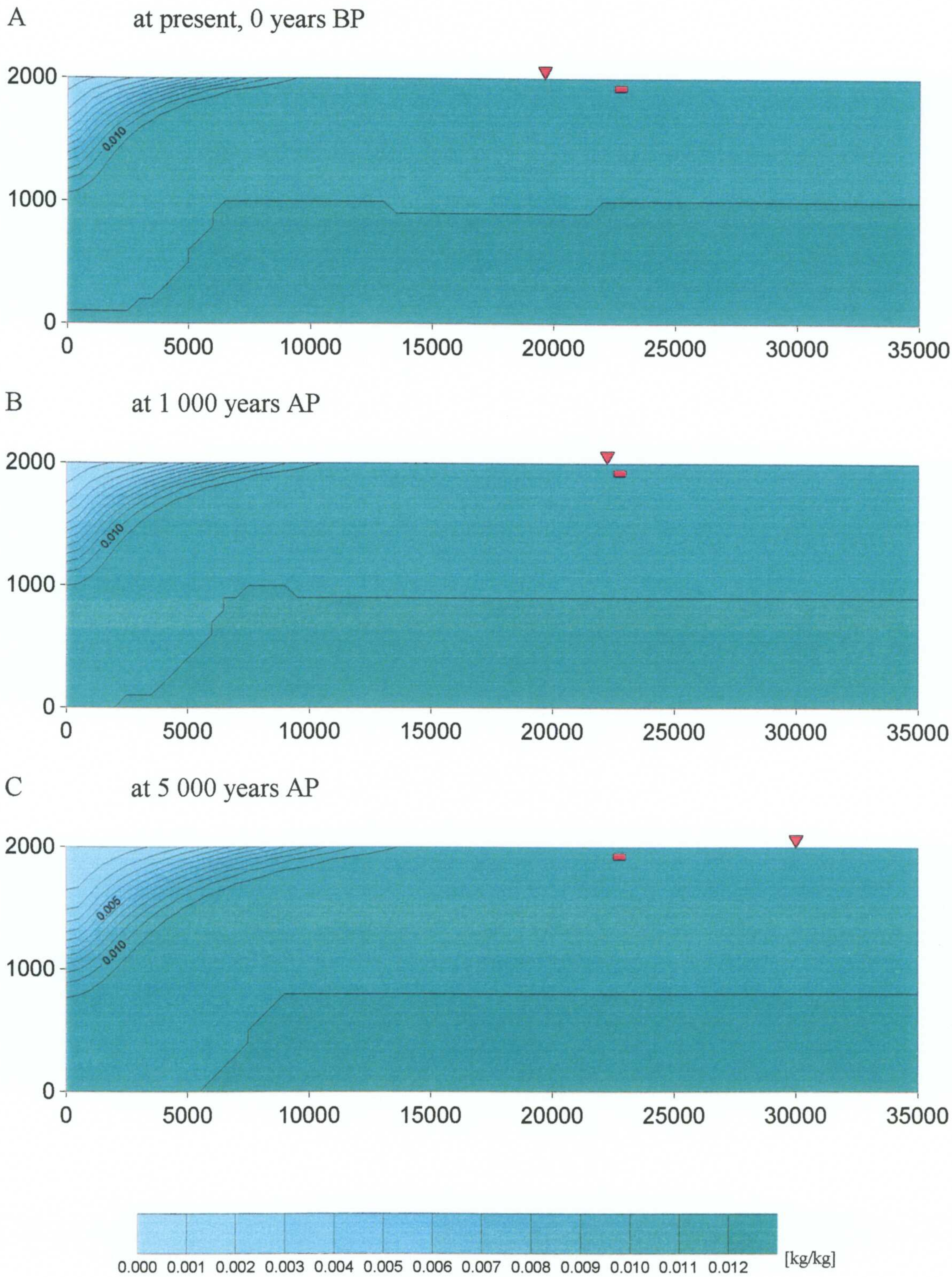

Figure 4-1. *Reference case with variable-density. Due to the low permeability the shoreline and the saltwater transition zone are not at the same location. SFR is marked with a square and the shoreline at the different times is marked with a triangle. Observe that the scale of the vertical axis is 5 times the horizontal.*

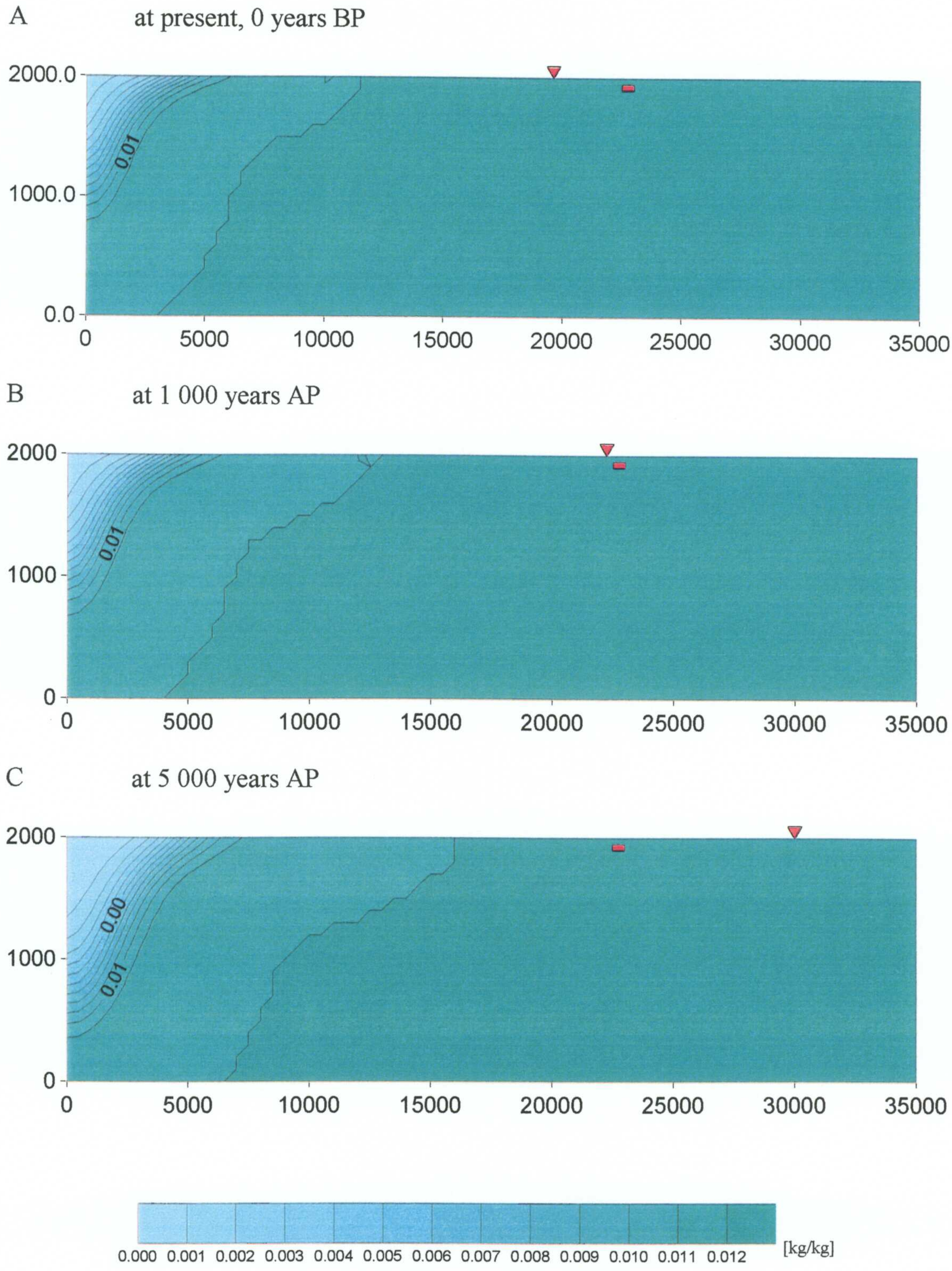

Figure 4-2. *Reference case with uniform-density. A comparison with Figure 4-1 shows that there are only minor differences in the location of the transition zone. SFR is marked with a square and the shoreline with a triangle. Observe that the scale of the vertical axis is 5 times the horizontal.*

4.2.2 Flow at the SFR

In Figure 4-3 the Darcy velocity and the angle of the flow through the element that corresponds to the SFR are plotted at every 1000 year. As long as the SFR is covered with water the flow is small and upward towards the sea bottom. When the coastline has passed, at about 1100-1200 years AP, the flow increases about 5 times and the flow changes direction so that it is parallel to the surface.

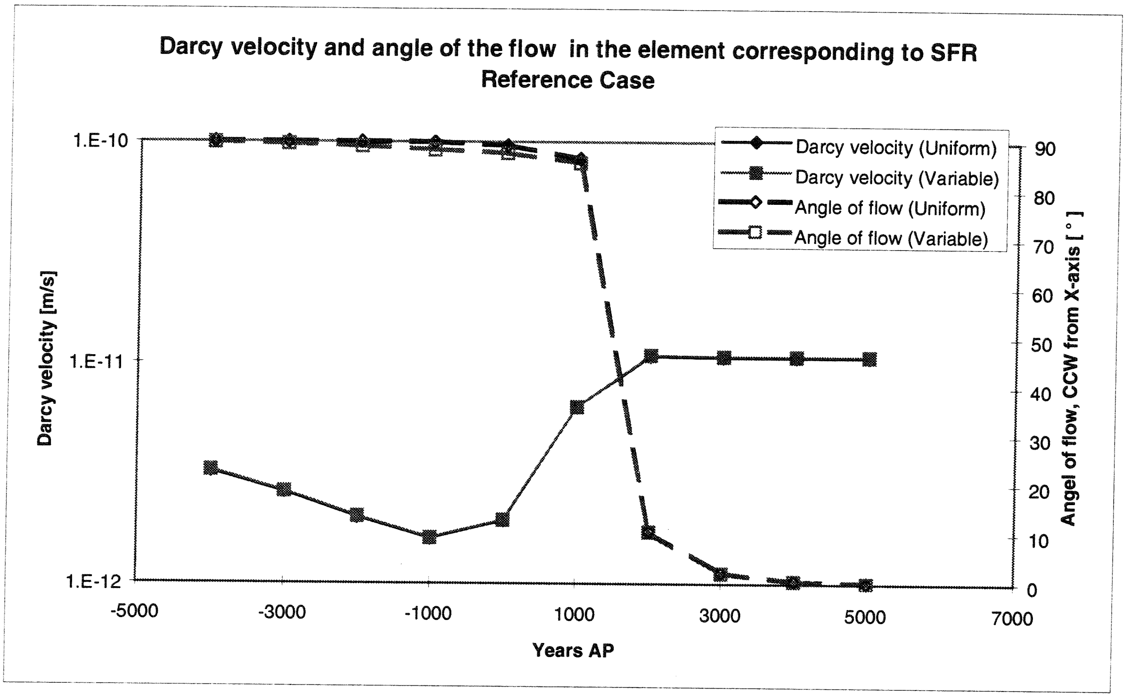

Figure 4-3. The magnitude and angle of the flow, for the reference case, through the element that corresponds to the SFR.

As can be seen in Figure 4-3, the conclusion from the homogenous reference model is that the differences in magnitude and direction of the Darcy velocity are negligible whether variable-density is taken into account or not.

4.3 Progress of salinity

A comparison between different rates of progress of salinity in the Baltic Sea is investigated to ensure that the progress not will have impact on the results.

The model is also homogeneous in this case. The permeability is set to $7 \cdot 10^{-16}$ m^2 and the porosity is 2‰. Accordingly no structures or layers are taken into account. The approach is to have one model with high gradient and one model with a low gradient of salinity decrease of the seawater. The first model begins with a salinity of 15‰ 5 000 years BP. The salinity decreases linearly to 5‰ at present and then continues to decrease to 2‰ 5 000 years into the future. The results are shown in Figure 4-4. In the other model, shown in Figure 4-5, the decrease in salinity is smaller. The model begins with a salinity of 12‰ that then decreases linearly to 5‰ at present and then remains at 5‰ into the future.

4.3.1 Salinity in the modelled profile

A comparison between Figure 4-4 and Figure 4-5 shows that differences between the appearance of the iso-lines of the concentration are negligible. Although there is a small difference throughout the simulated time, the fresh water will penetrate deeper into the bedrock and will extend a shorter distance to the Baltic for the case with more constant evolution of seawater salinity, see Figure 4-5. In this case, the saline water is less heavy due to lower concentration of salinity and in accordance with the conclusions in section 4.2 the fresh water will penetrate deeper into the bedrock.

Another result of this run is that if the salinity of the sea water decreases or is maintained constant into the future, it does not have an impact on the transition zone in the model, c.f. Figure 4-1 and Figure 4-5.

The conclusion is that the progress of salinity does not impact the spatial concentration of salt around SFR.

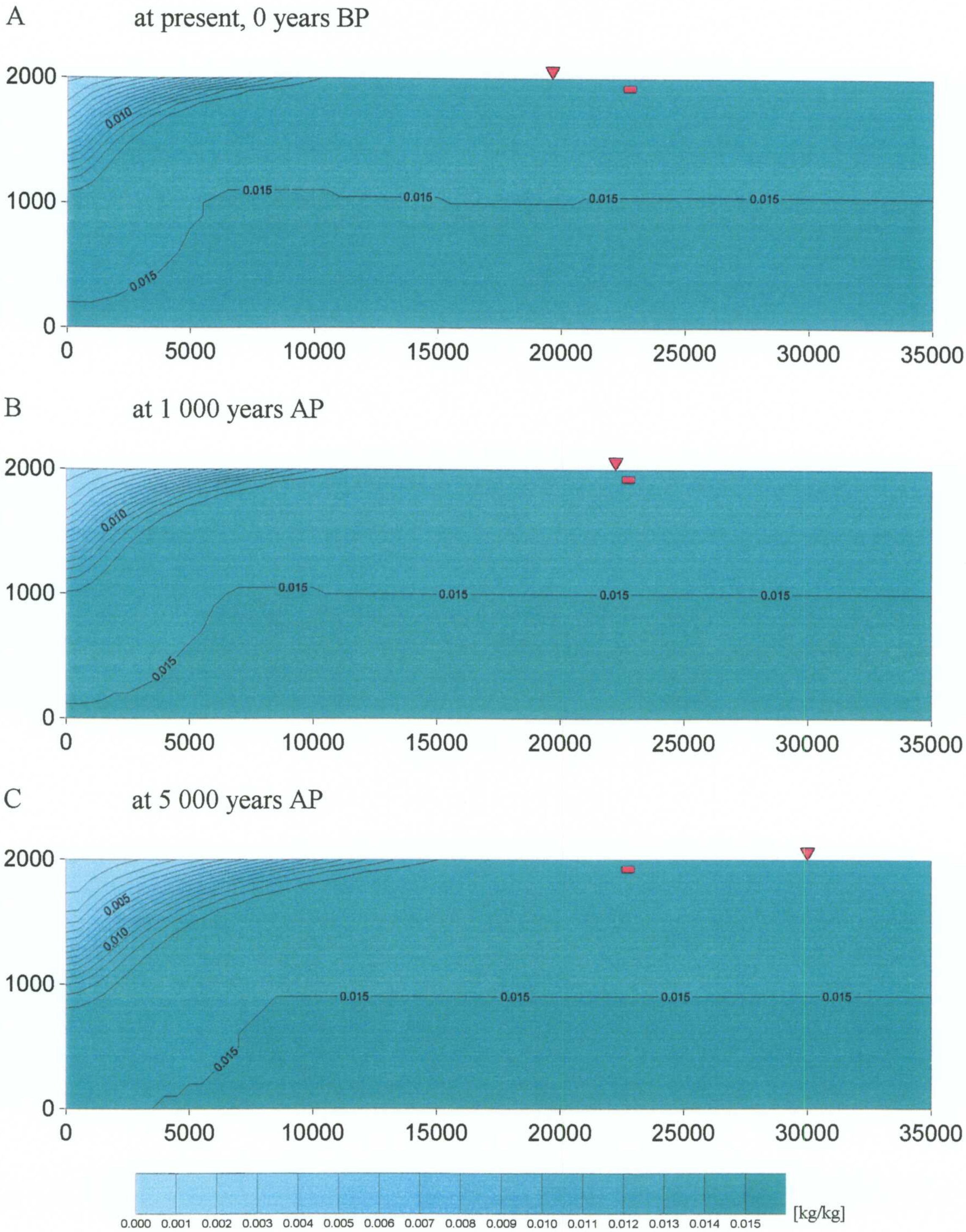

Figure 4-4. *Homogenous model with a large difference between the initial, 15‰, and the final, 2‰, salinity of the water in the Baltic Sea. SFR is marked with a square and the shoreline with a triangle. Observe that the scale of the vertical axis is 5 times the horizontal.*

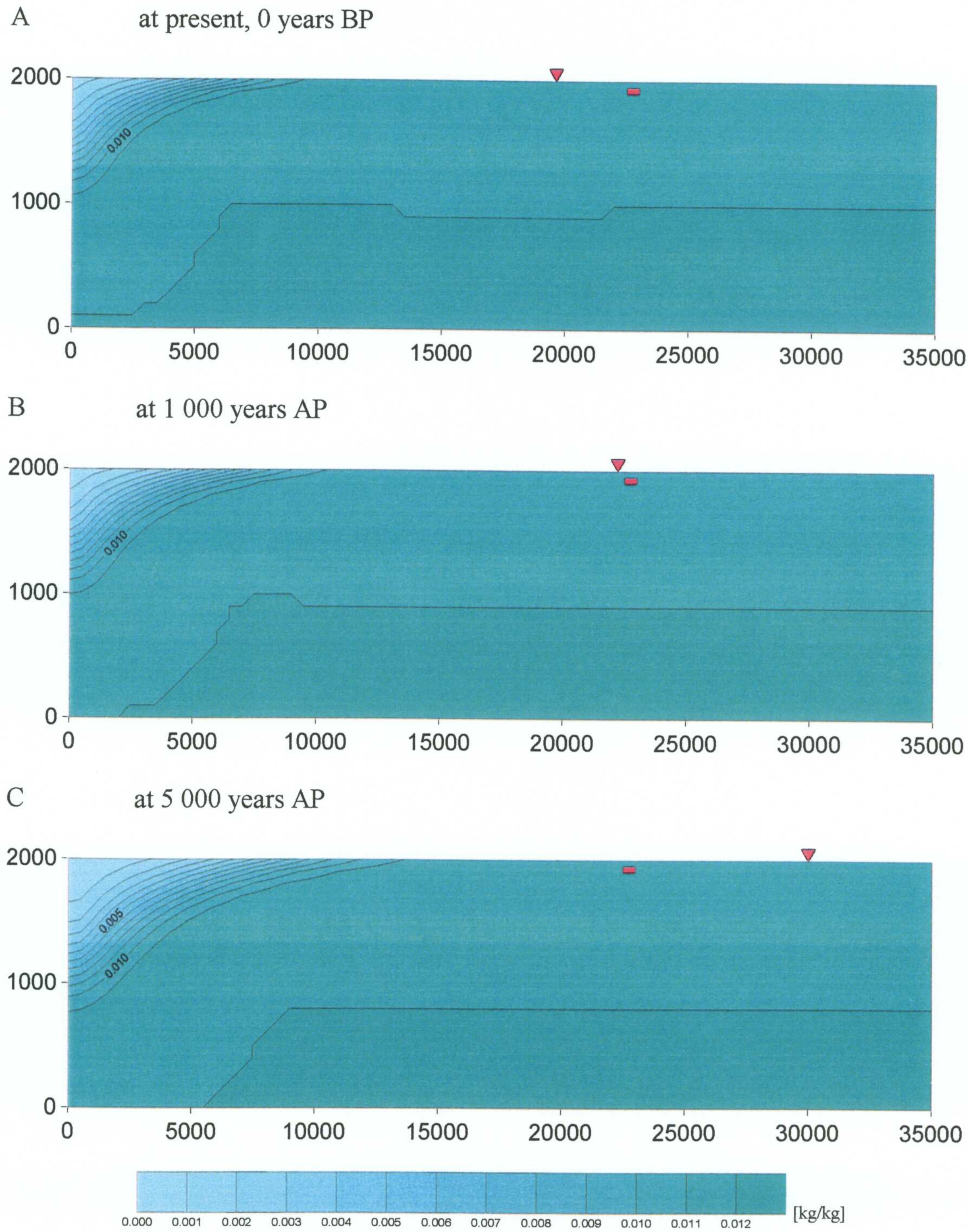

Figure 4-5. *Homogenous model with small difference between the initial and the final salinity of the water in the Baltic Sea, 12‰ and 5‰ respectively. Comparison with Figure 4-1 shows that the future evolution of salinity does not impact on the transition zone. SFR is marked with a square and the shoreline with a triangle. Observe that the scale of the vertical axis is 5 times the horizontal.*

4.3.2 Flow at the SFR

The Darcy velocity and angle of the flow through SFR are shown in Figure 4-6. The magnitude of the flow is small and upward as long as SFR is covered by seawater. When the shoreline passes, the flow increases about 5 times and the flow becomes parallel to the surface.

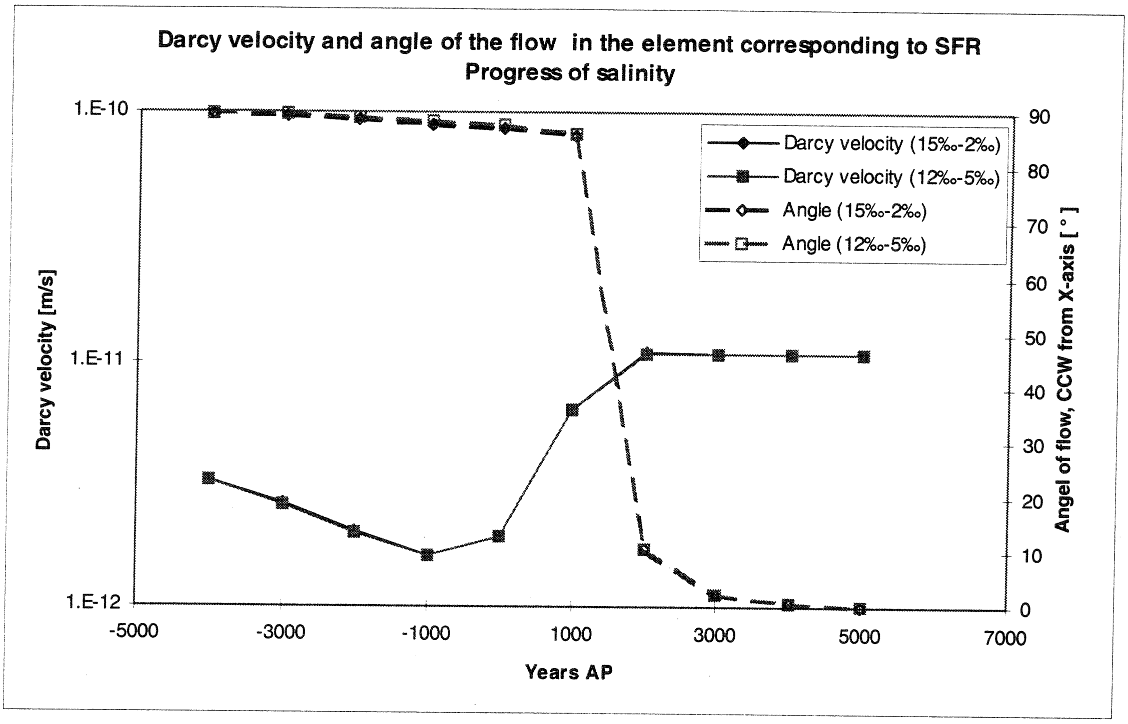

Figure 4-6. *The magnitude and angle of the flow, for the case with progress in salinity, through the element that corresponds to the SFR.*

According to Figure 4-6 and Figure 4-3 the progress of salinity of the seawater is of minor importance and will not impact the flow of the groundwater at the SFR.

4.4 High permeability in surface layer

As suggested by Axelsson and Hansen (1997) that the uppermost of the bedrock around SFR has a higher permeability than the lower parts of the bedrock, a model with a high permeable layer is thus investigated.

For this case, the evolution of seawater salinity is described by 15‰ at 5 000 years BP, 5‰ today and then remains constant into the future. No structures are taken into account and the porosity is set to be 2‰ throughout the modelled domain. The permeability of the bedrock is $7 \cdot 10^{-16}$ m^2, Except for the upper 200 m. In this uppermost layer the permeability is increased 100 times to $7 \cdot 10^{-14}$ m^2.

4.4.1 Salinity in the modelled profile

Two different flow regions will occur in this modell, an upper fast motion in the highly permeable layer, and a slow motion in the lower region. Both of these two regions show the same phenomena as explained in section 4.2, i.e. when variable-density is taken into account, see Figure 4-7, the fresh water flows on the top of the saline water and it will not flush as deep as the fresh water shown in Figure 4-8. However the effect is even smaller in the upper 200 m.

In both cases the results show that most of the flow will occur in the upper highly permeable layer, see Figure 4-7 and Figure 4-8. In the upper layer the location of the transition zone is at the same place in both simulations. The transition zone in this model is located at the same place as the shoreline, this is preferable since it coincides with what is observed in the field.

The most important conclusion from this model is that the spatial differences that occur in salinity due to variable-density are minor as compared to the impact that the highly permeable layer has on the spatial variation of salinity. The line 15‰ does differ between the two realisations. This depends on that there will be almost no flow in the low permeable bedrock when variable-density is assumed. However this does not matter since the SFR is situated only 50 m below the rock surface.

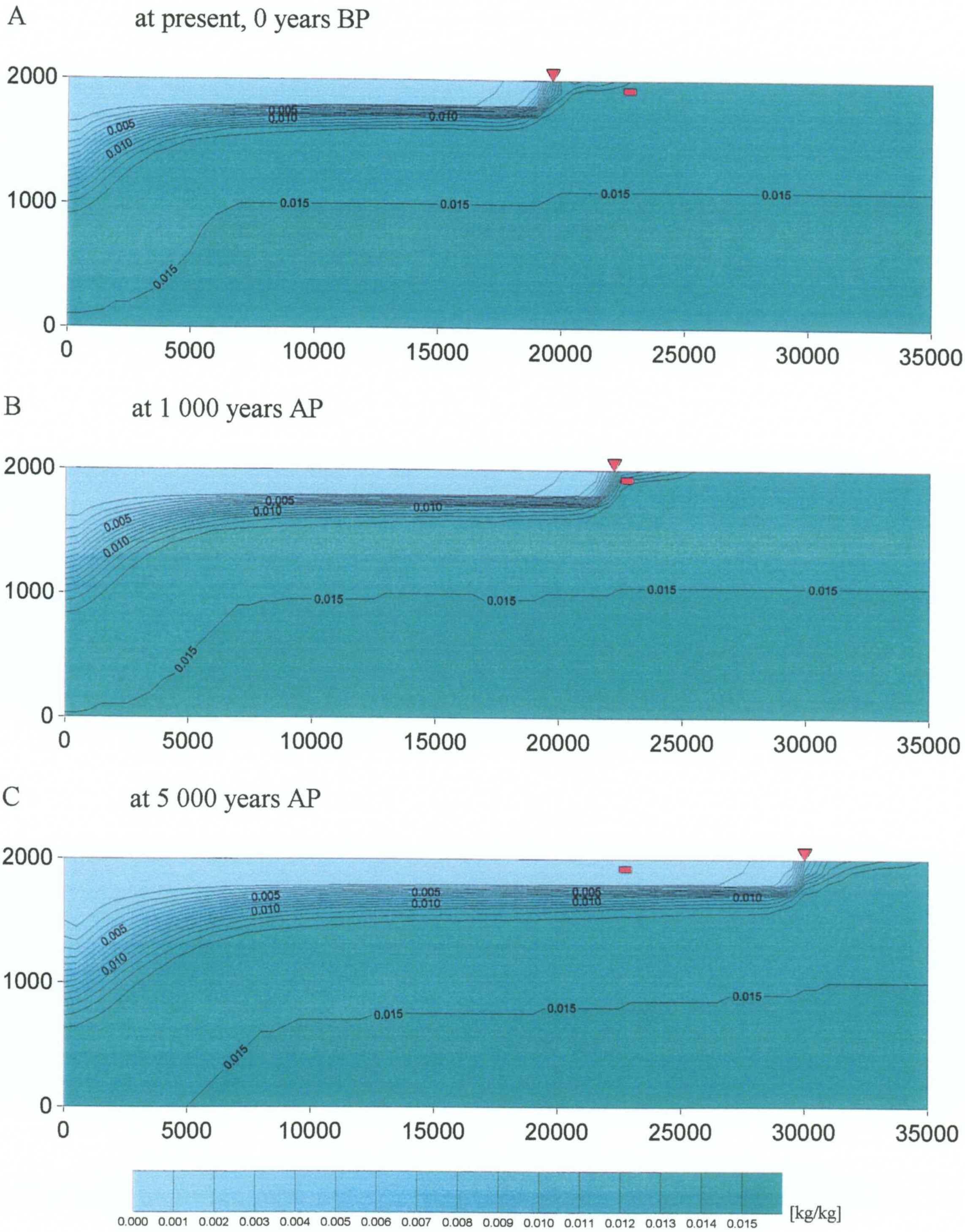

Figure 4-7. *Case with variable-density and high permeable layer. The transition zone coincides with the shoreline (the triangle). Two flow regions occur, one fast in the upper high permeable layer and one slow in the low permeable bedrock. SFR is marked with a square. Observe that the scale of the vertical axis is 5 times the horizontal.*

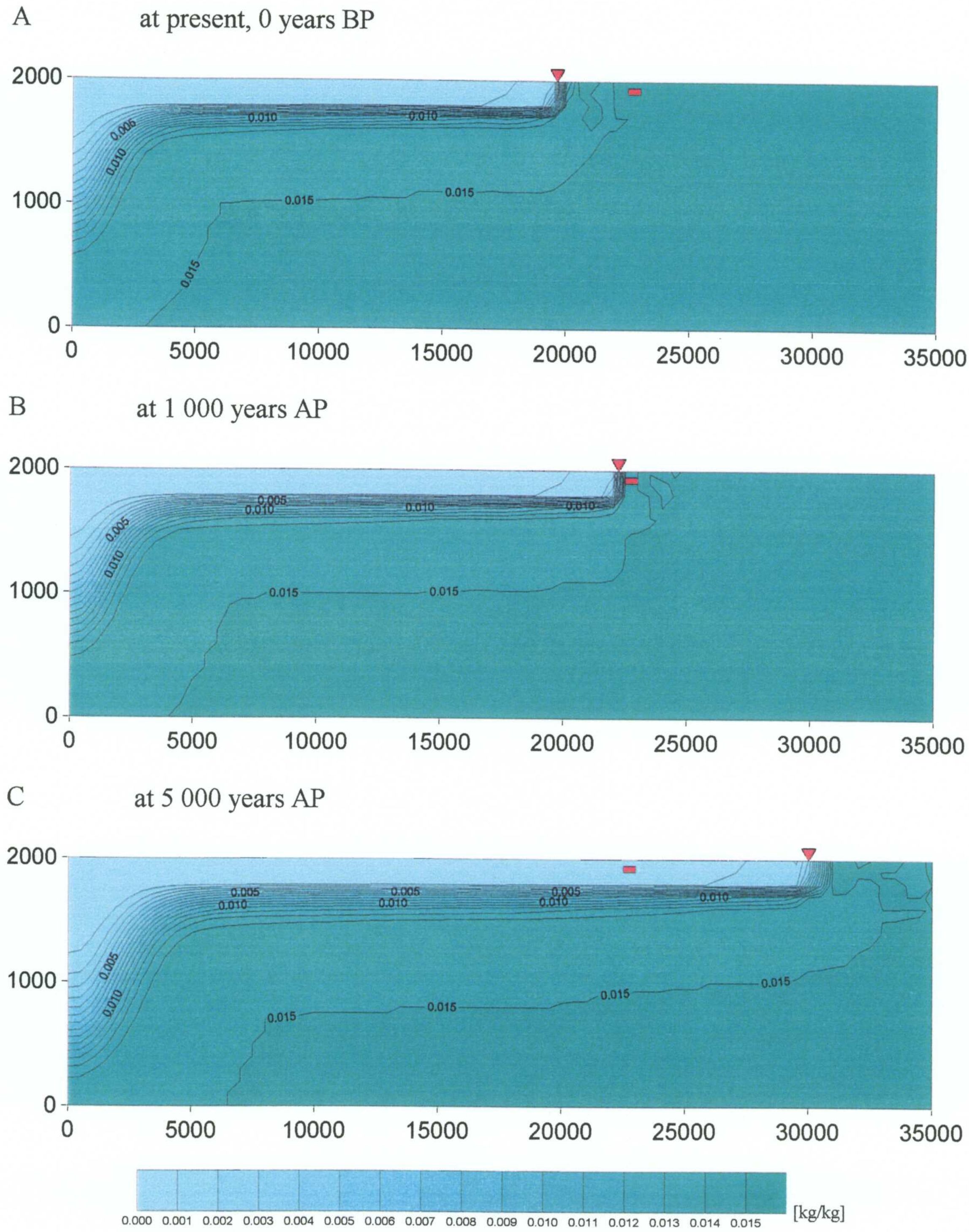

Figure 4-8. *Uniform-density and high permeable surface layer. Two flow regions occur. A fast in the surface layer and a slow in the low permeable region. A comparison with Figure 4-7 shows that there are only small spatial differences in the concentration of salt between the two models. SFR is marked with a square and the shoreline with a triangle. Observe that the scale of the vertical axis is 5 times the horizontal.*

4.4.2 Flow at the SFR

When a high permeable surface layer is assumed some differences occur in the flow at the SFR. As shown in Figure 4-9 the flow will be larger if variable-density is assumed as long as the SFR is covered with seawater. On the other hand the flow will be steeper towards sea bottom if uniform-density is assumed during the same time period. As soon as the shoreline has passed the SFR, 1100-1200 years AP, the flow will increase 400 times and the flow will be parallel to the surface.

A comparison between Figure 4-9 and Figure 4-3 shows that the Darcy velocity is almost the same as long as the SFR is under the sea, but then, after the shoreline has withdrawn, the flow in the high permeable layer becomes approximately 100 times larger than in the reference case.

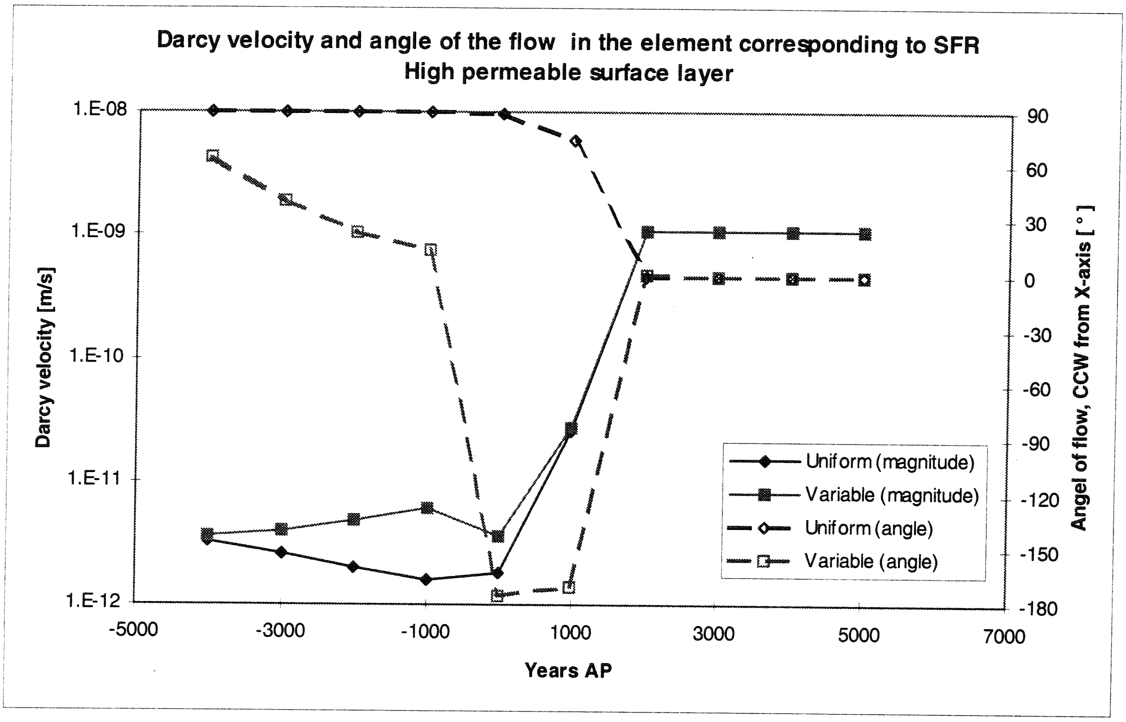

Figure 4-9. The magnitude and angle of the flow through the element that corresponds to the SFR for the case with a high permeable surface layer.

The differences in magnitude and angle of the flow counteract each other so that the transport time for the water from the SFR to the sea bottom will be slightly longer, the difference is less than 1.5%, if uniform-density is assumed. The most important conclusion is that as soon as the shoreline has passed the SFR the magnitude and the angle of the flow become the same whether a uniform-density or a variable-density approach is assumed.

4.5 Correlated porosity to hydraulic conductivity

It is possible that there is a correlation between increasing permeability and increasing porosity. This case is modelled to investigate the impact this correlation will have on the groundwater flow.

This model has an evolution in seawater salinity that is described by a salinity of 15‰ at 5 000 years BP and 5‰ from present and 5 000 years into the future. No structures are taken into account, but the upper 200 m are set to have a permeability that is increased 100 times and a porosity that is increased 10 times compared to the underlying bedrock. The permeability in this layer is $7 \cdot 10^{-14}$ m^2 and the porosity is 2%, consequently the rest of the modelled domain has a permeability that is $7 \cdot 10^{-16}$ m^2 and a porosity that is 2‰.

4.5.1 Salinity in the modelled profile

Figure 4-10 and Figure 4-11 show the results from this model. The only spatial difference in salinity between this case and the case presented in section 4.4 is that the transition zone is no longer at the shoreline. This depends both on that the transport time and that the amount of saline water that has to be washed out to the Baltic Sea increases with the porosity. Accordingly the flow is determined by the highly permeable layer and most of the flow will occur in this layer. Not much flow will occur in the lower region.

The conclusion from the model is that the porosity has a large impact on the results while it does not matter if the salinity is assumed density dependent or if it is assumed to only be a tracer. The impact on the flow and salinity around SFR will once again only be a translation in time when the transition zone hits the target area.

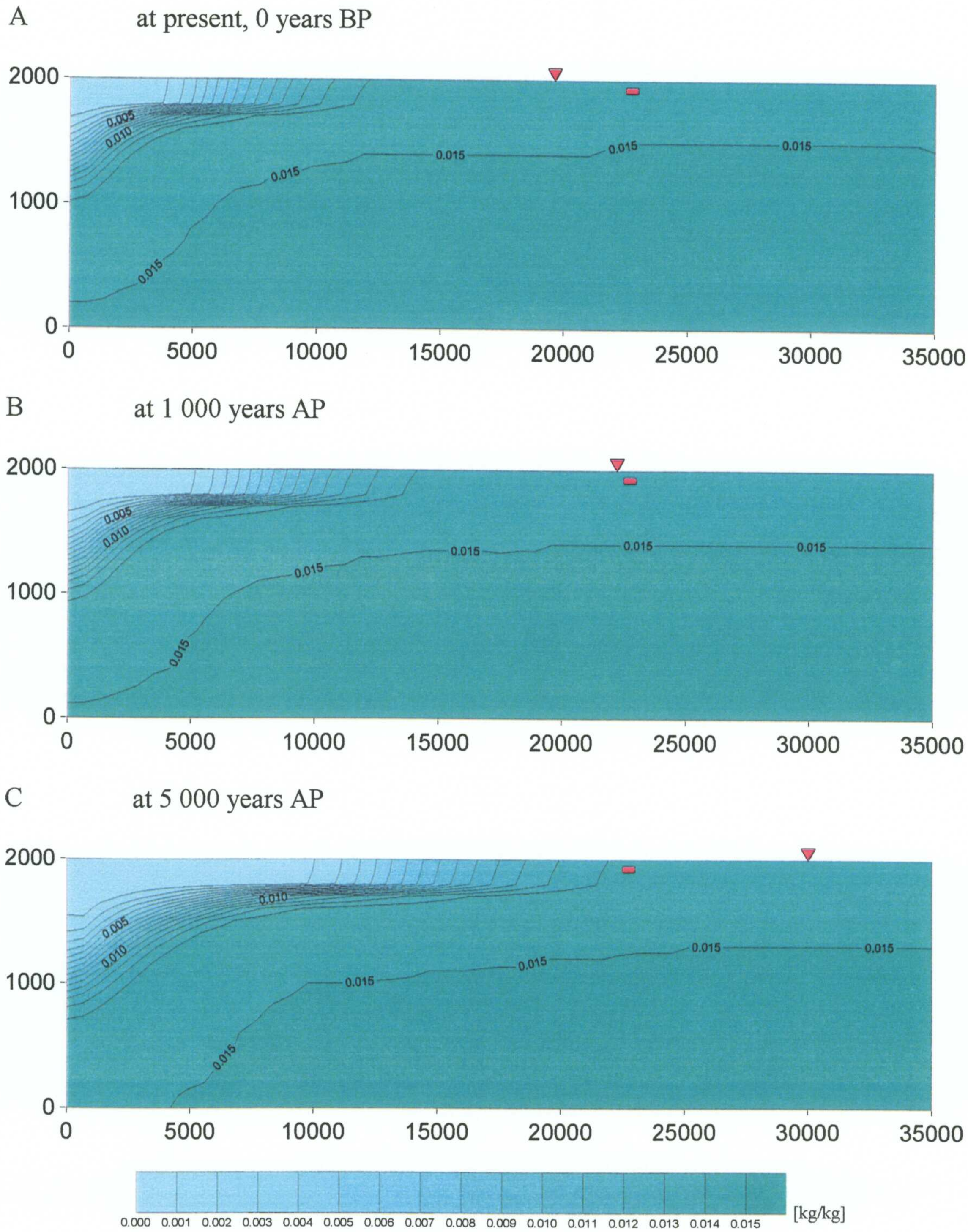

Figure 4-10. *High permeable and high porous surface layer and variable-density. The only spatial difference in salinity between this case and the case with only high permeable layer, c.f. Figure 4-7, is that the upper layer is more saline depending on that the transport time and the volume of saline water increase with porosity. SFR is marked with a square and the shoreline with a triangle. Observe that the scale of the vertical axis is 5 times the horizontal.*

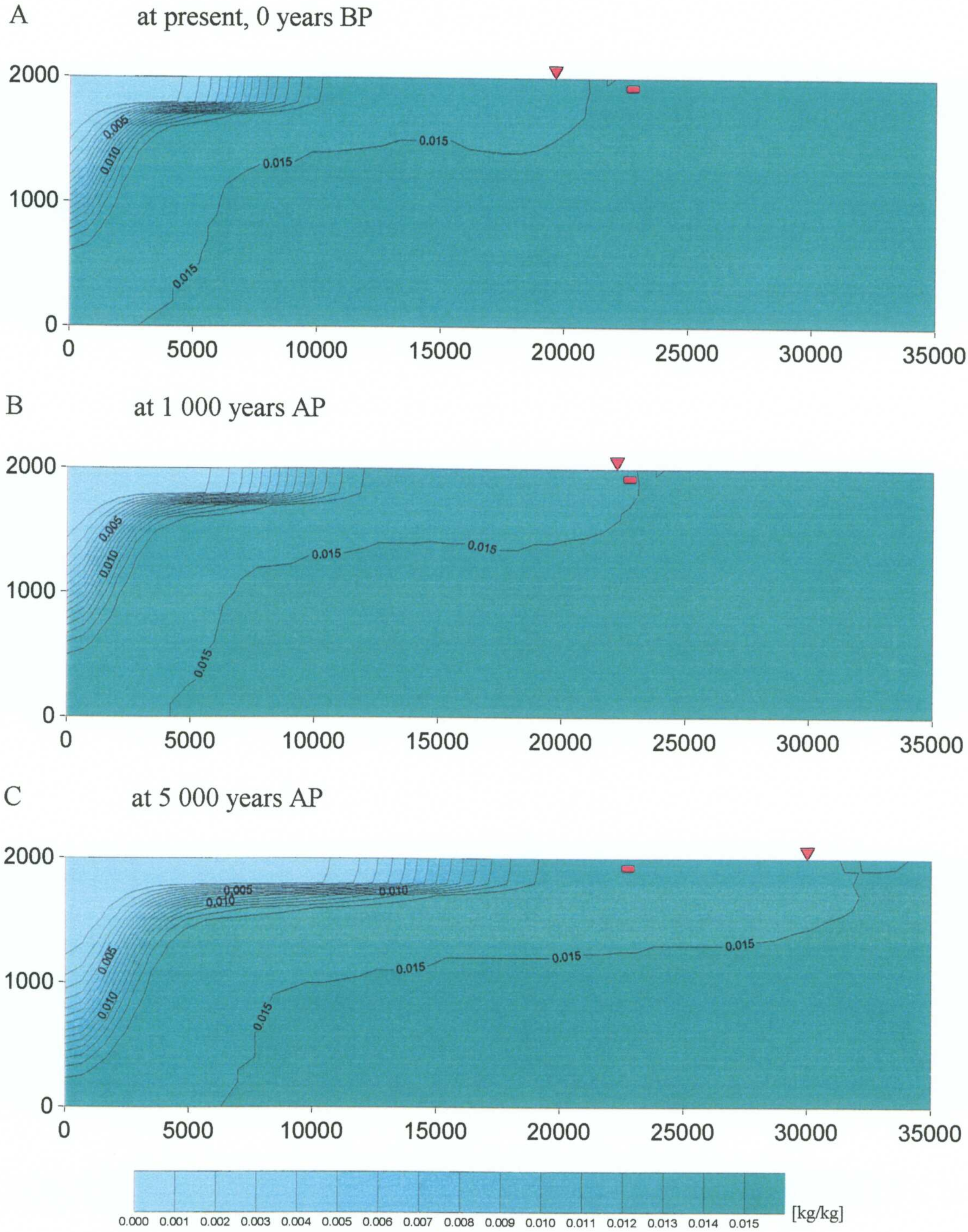

Figure 4-11. *High permeable surface layer with increased porosity and uniform-density. Comparison with Figure 4-10 shows that there are only minor spatial differences in salinity if variable-density is taken into account or if the salt is modelled as a tracer. SFR is marked with a square and the shoreline with a triangle. Observe that the scale of the vertical axis is 5 times the horizontal.*

4.5.2 Flow at the SFR

When the porosity is increased 10 times in the high permeable surface layer there are some differences in the flow. Figure 4-12 shows that the Darcy velocity will be larger when the density effect is taken into account, as long as the shoreline has not passed the SFR. The direction of the flow is more upwards towards sea bottom when the uniform-density is assumed. When the shoreline has withdrawn such that land is above the SFR the flow increases 200-400 times while the direction of the flow becomes parallel to the ground surface.

A comparison between Figure 4-12 and Figure 4-9 shows that the Darcy velocity is almost the same. The differences in magnitude and direction of the flow for the two different approaches are smaller when the porosity is correlated to the permeability.

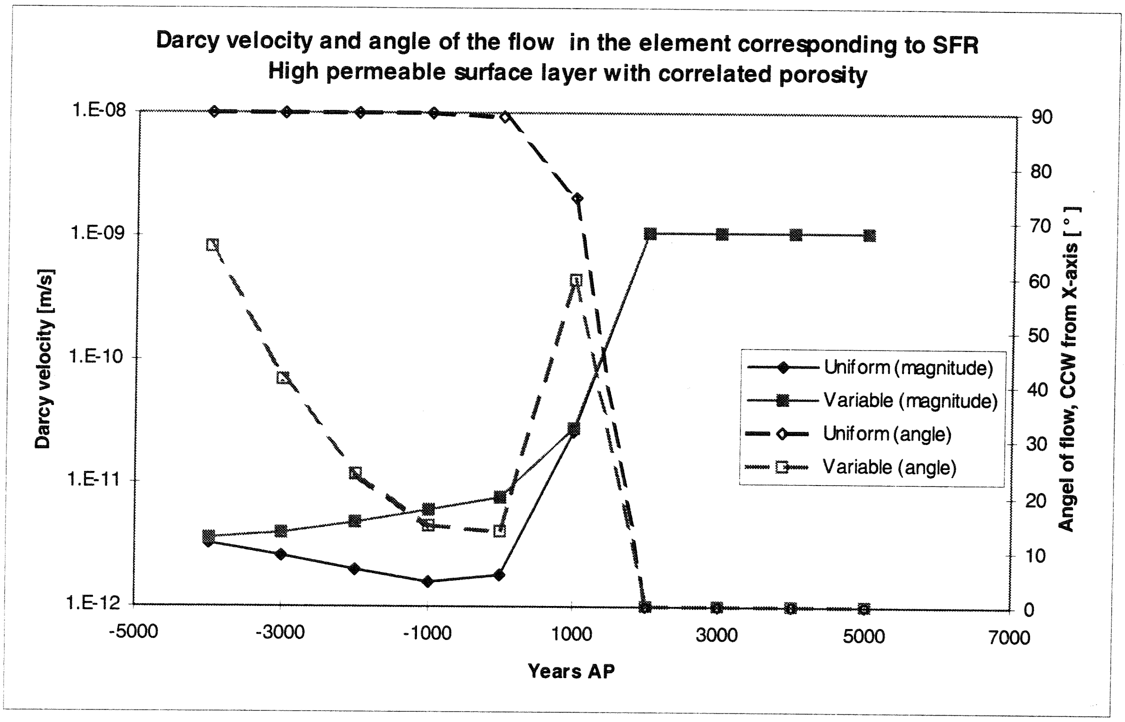

Figure 4-12. The magnitude and angle of the flow through the element that corresponds to the SFR for the case with porosity correlated to permeability.

The differences in magnitude and direction counteract each other so that the difference in transport time for the water that flows from the SFR to the sea bottom is only 1.5% longer if the uniform-density is assumed. Most important is, though, that as soon as the shoreline has passed the SFR the differences in direction and magnitude for the flow are negligible.

4.6 High permeable vertical structures

The effect of the two major vertical structures in the region of the SFR is studied in order to investigate the impact that vertical structures will have on the flow.

The permeability is set to $7 \cdot 10^{-16}$ m^2 throughout the model domain with exception of the vertical structures where the permeability is $7 \cdot 10^{-14}$ m^2. The structures are located at 16 500 m, corresponding to the Forsmark zone, and at 22 200 m, corresponding to the Singö zone. The porosity of the bedrock, 2‰, is kept constant in the model domain, also in the structures. The Progress of the salinity in the sea water starts with an initial value of 15‰ at 5 000 years BP, it then decreases to 5‰ at present and remains at this value for the next 5 000 years.

4.6.1 Salinity in the modelled profile

A comparison between Figure 4-13, where variable-density is taken into account, and Figure 4-14, where the groundwater density is constant, shows that the flushing depths in the zones are almost the same for the different approaches. There is however a spatial difference in salinity in the horizontal extension of the freshwater. In the case where variable-density is taken into account, Figure 4-13, the fresh water will extend further horizontally than for the case with constant density, Figure 4-14. This is because the fresh water flows on the top of the saline.

The conclusion from this case is that highly permeable structures make the spatial differences in salinity between the two density approaches negligible, i.e. the more complex the model is the minor the differences become.

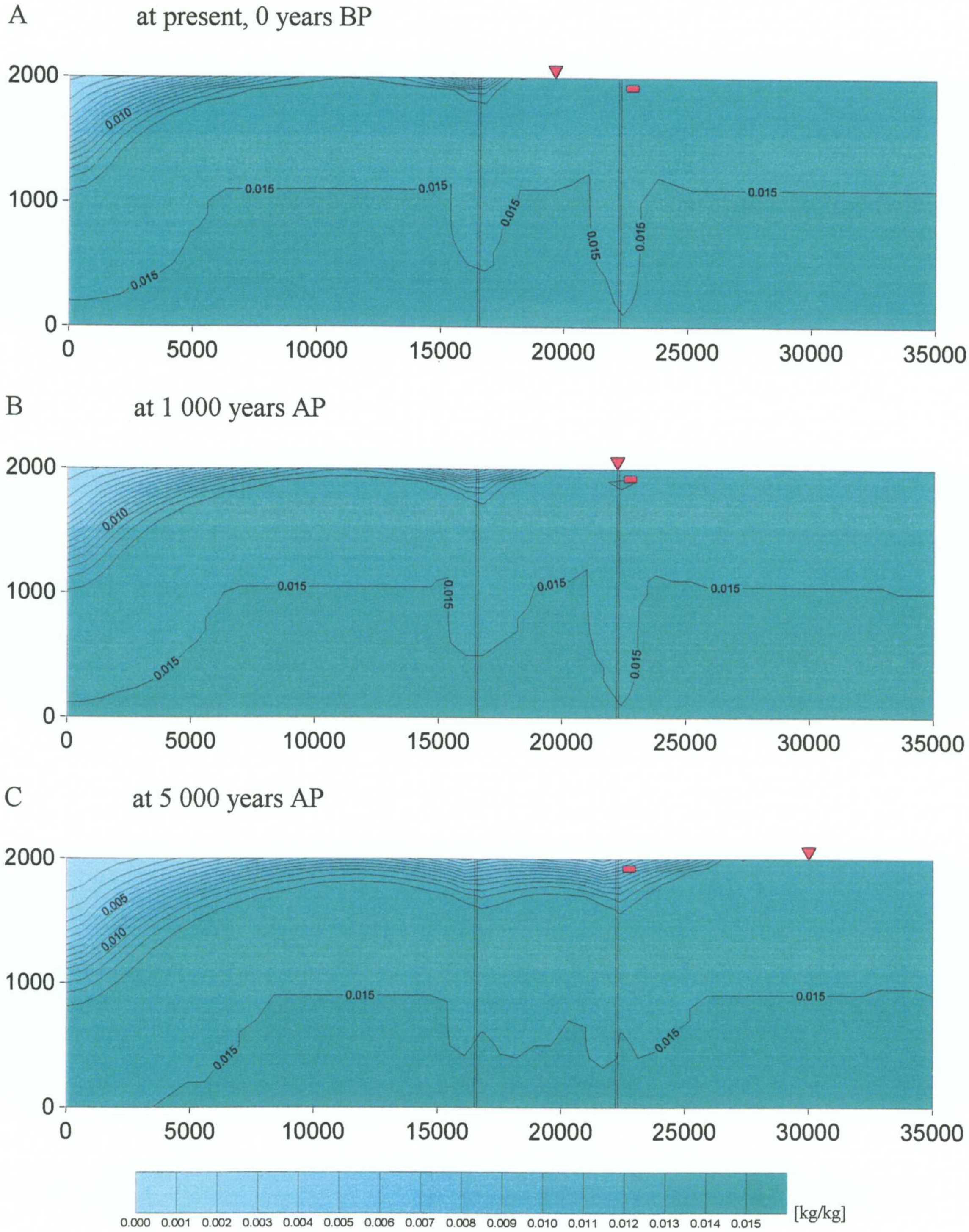

Figure 4-13. *Case with high permeable vertical structures and variable-density. Fresh water will flush the zones when the shoreline has withdrawn. SFR is marked with a square and the shoreline with a triangle. The zone at 16 500 m corresponds to The Forsmark zone while the Singö zone is situated at 22 200 m. Observe that the scale of the vertical axis is 5 times the horizontal.*

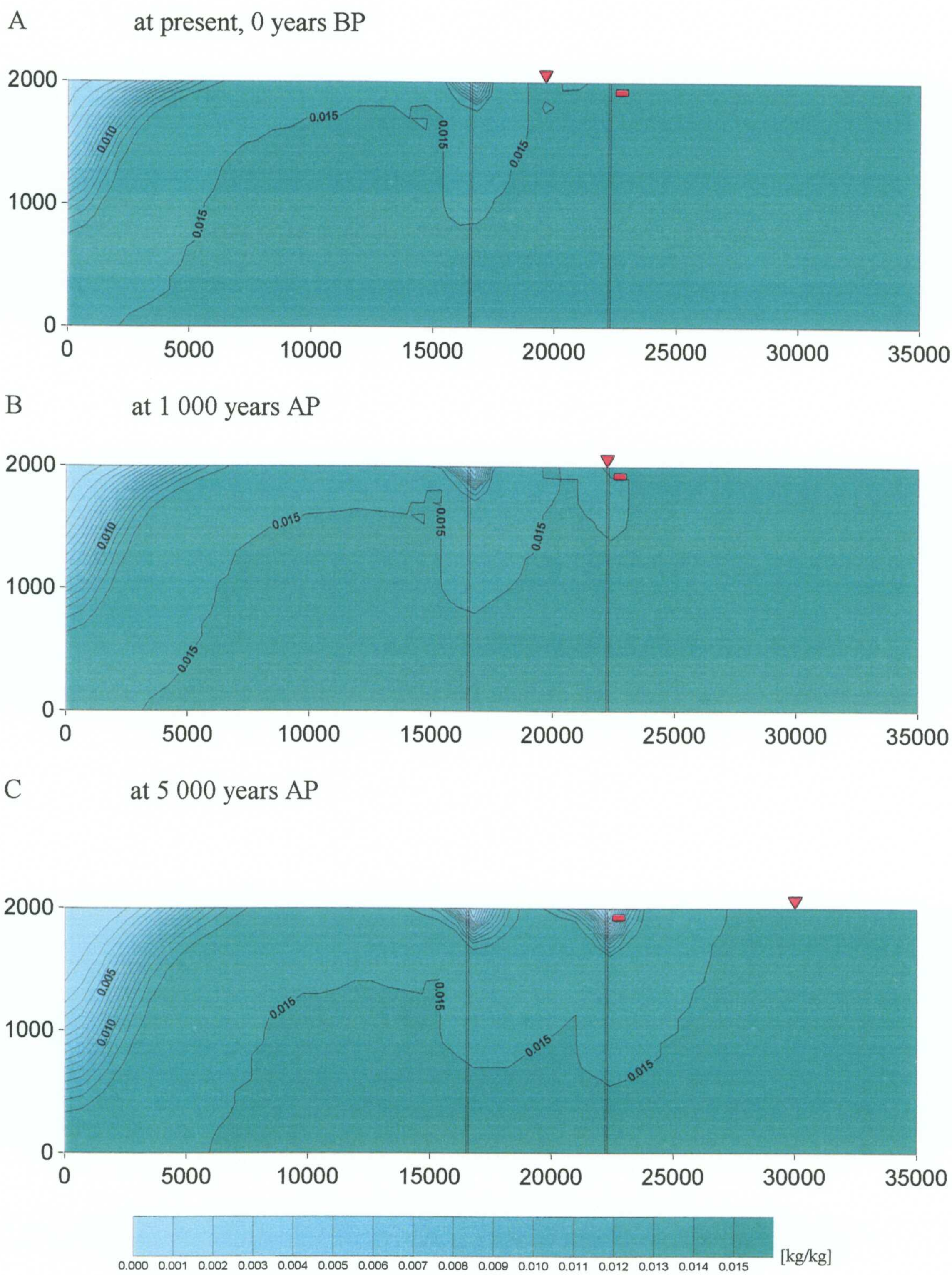

Figure 4-14. *Uniform-density and high permeable vertical zones. The concentration of salt is greatly affected by the zones. There are some differences in salinity between the two different approaches, c.f. Figure 4-13, but in comparison to what the zones do for the salinity, c.f. Figure 4-2, the spatial differences in salinity are minor. The zone at 16 500 m corresponds to The Forsmark zone while the Singö zone is at 22 200 m. The vertical axis is 5 times the horizontal*

4.6.2 Flow at the SFR

Only small differences in magnitude and direction of the flow occur when high permeable vertical structures are implemented into the model. During the time that the SFR is under the Baltic Sea the magnitude of the flow is almost the same, while the direction is slightly more upwards when a uniform-density approach is used, see Figure 4-15. After the shoreline has withdrawn the flow increases about 10 times. The increase is slightly larger for the uniform-density approach. The direction of the flow will be more horizontal, but for the uniform-density there will remain a slight angel upwards. For the variable-density approach the direction will be slightly downwards after the shore line has passed, but this flow downwards will decrease and be parallel to the surface at the end of the simulated time.

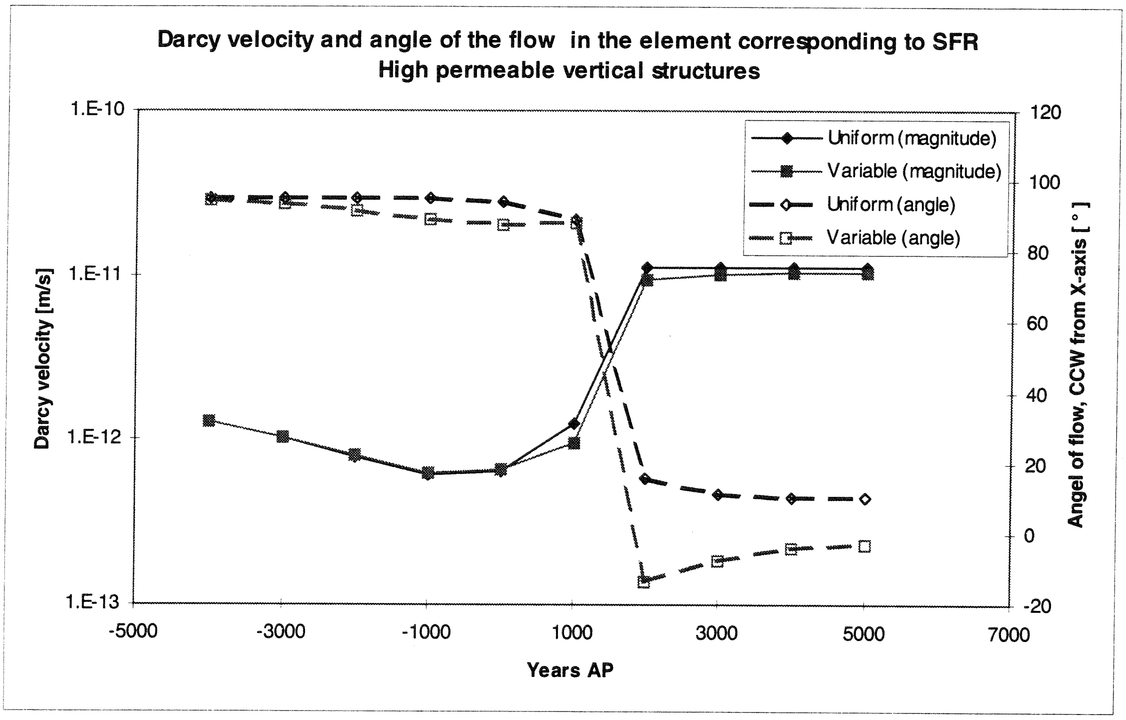

Figure 4-15. The magnitude and angle of the flow through the element that corresponds to the SFR for the case with high permeable vertical structures.

The groundwater flow through the SFR is greater for the uniform-density case. That is the Darcy velocity is larger and the direction of the flow is more upwards. Hence the simulated transport time between the SFR and the surface will be shorter for the uniform-density case than for the variable density case.

4.7 Low permeable vertical structures

As a comparison to the highly permeable structures an investigation of low permeability structures is made.

In the vertical structures the permeability is decreased 100 times in comparison to the surrounding bedrock. Accordingly the permeability is $7 \cdot 10^{-18}$ m^2 in the structures and $7 \cdot 10^{-16}$ m^2 in the rest of the modelled domain. The porosity is 2‰ throughout the model, while the salinity initially is 15‰ at 5 000 years BP and from present and 5 000 years into the future it is assumed to be constant at 5‰. The structures are located at 16 500 m and at 22 200 m, see Figure 4-16 and Figure 4-17.

4.7.1 Salinity in the modelled profile

As can be seen in Figure 4-16 and in Figure 4-17 the zones in this model act as dense shields that stem the flow of saline groundwater towards the Baltic Sea. The water is forced towards the surface in front of each zone. Behind every zone, acting as a no-flow boundary, a new flush of fresh water will occur downwards in the bedrock. The appearance of the fresh water intrusion, behind these shields, looks like the upper vertical boundary, i.e. the fresh water will flush deeper if no density effect is taken into account, while it will reach further towards the Baltic Sea if variable density is taken into account.

The conclusion is that the impact on the SFR will be practically the same if density is assumed to be constant or correlated to the salinity.

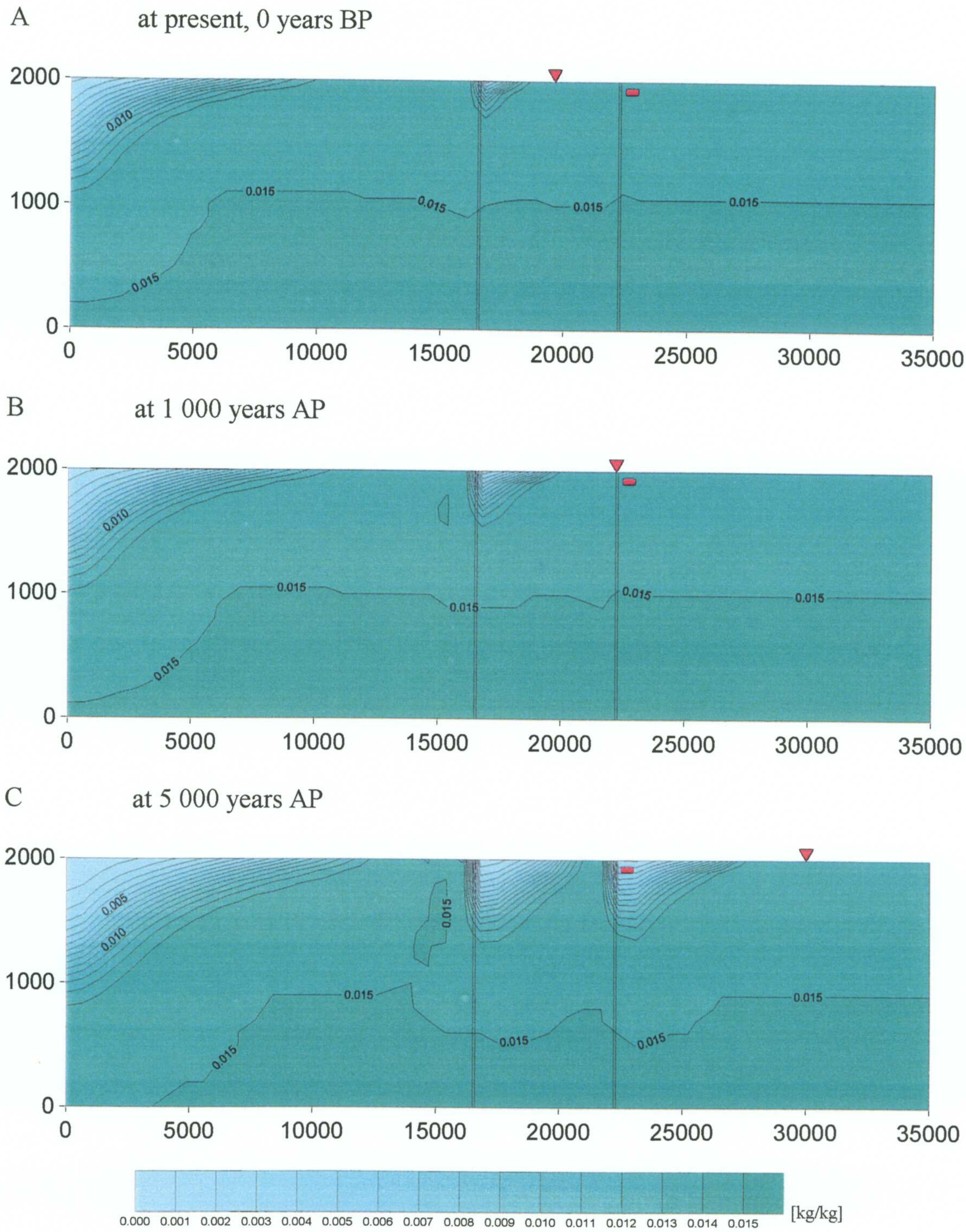

Figure 4-16. *Case with two low permeable vertical structures and variable-density. The zones act as dense shields, almost like a no-flow boundary. SFR is marked with a square and the shoreline with a triangle. The zone at 16 500 m corresponds to The Forsmark zone while the Singö zone is situated at 22 200 m. Observe that the scale of the vertical axis is 5 times the horizontal*

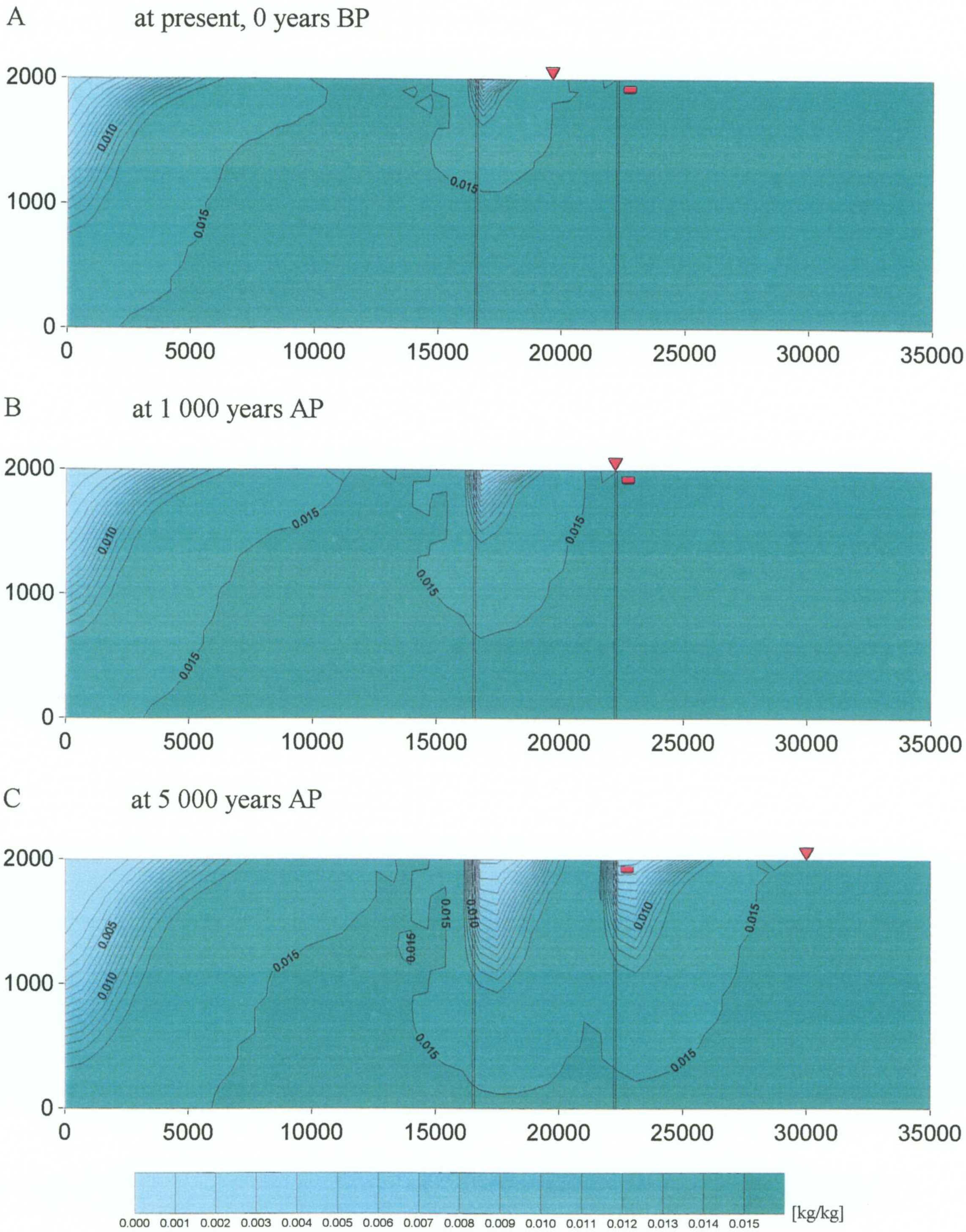

Figure 4-17. *Uniform-density case with low permeable vertical structures. The spatial differences in salinity that occur between the uniform-density approach and the variable-density approach, c.f. Figure 4-16, is the same as explained in section 4.2. SFR is marked with a square and the shoreline with a triangle. The zone at 16 500 m corresponds to The Forsmark zone while the Singö zone is situated at 22 200 m. Observe that the scale of the vertical axis is 5 times the horizontal*

4.7.2 Flow at the SFR

As long as the SFR is under the sea bottom the magnitude and the angle of the flow will be almost the same whether variable-density or uniform-density is taken into account, c.f. Figure 4-18. When the shoreline has passed over the SFR the Darcy velocity increases 8 times. The direction of the flow changes from being upward to be slightly downwards, for the variable-density approach the angle is 30°-35° downward while it is about 50° for the uniform-density approach.

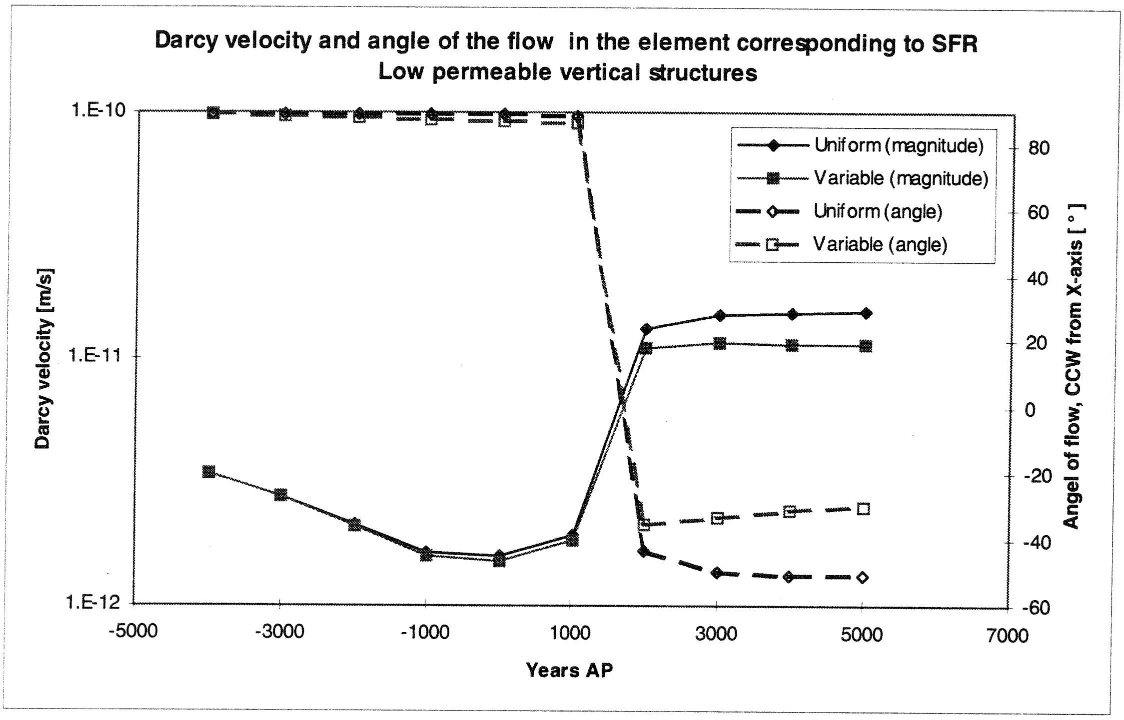

Figure 4-18. *The magnitude and angle of the flow through the element that corresponds to the SFR for the case with low permeable vertical structures.*

The main conclusion from the model with low permeable vertical structures is that the flow will be about 40% larger for the uniform-density approach, but it will be downwards into the bedrock.

4.8 Horizontal and vertical structures

Since the result from a single horizontal structure is almost the same as for the case with a highly permeable surface layer, see section 4.4, the case is not shown. Instead the interplay between vertical and horizontal structures is shown.

The permeability in the structures is $7 \cdot 10^{-14}$ m^2 while the permeability of the surrounding bedrock is $7 \cdot 10^{-16}$ m^2. Throughout the model domain the porosity is set to 2‰. The evolution of salinity in the seawater is 15‰ at 5 000 years BP, 5‰ at present and 5‰ at 5 000 years AP. The vertical zones are located at 16 500 m and at 22 200 m, corresponding to the Forsmark zone and the Singö zone respectively. The horizontal structure, corresponding to the H2 zone, is placed at a depth of 125-150 m and reaches across the whole model, see Figure 4-19 and Figure 4-20.

4.8.1 Salinity in the modelled profile

When the complexity of the model is increased the flow will be guided by the structures in the model, c.f. Figure 4-19 and Figure 4-20. In both cases the flow will be guided by the horizontal structure while the effect from the vertical structures can only be seen in the parts that are above the horizontal structure. This depends on the fact that the fresh water flows along the path that has the smallest resistance.

The conclusions from this model are that the appearance of vertical structures is very important for the flow and salinity, and that the impact on the SFR will be the same whether variable-density or uniform-density is assumed.

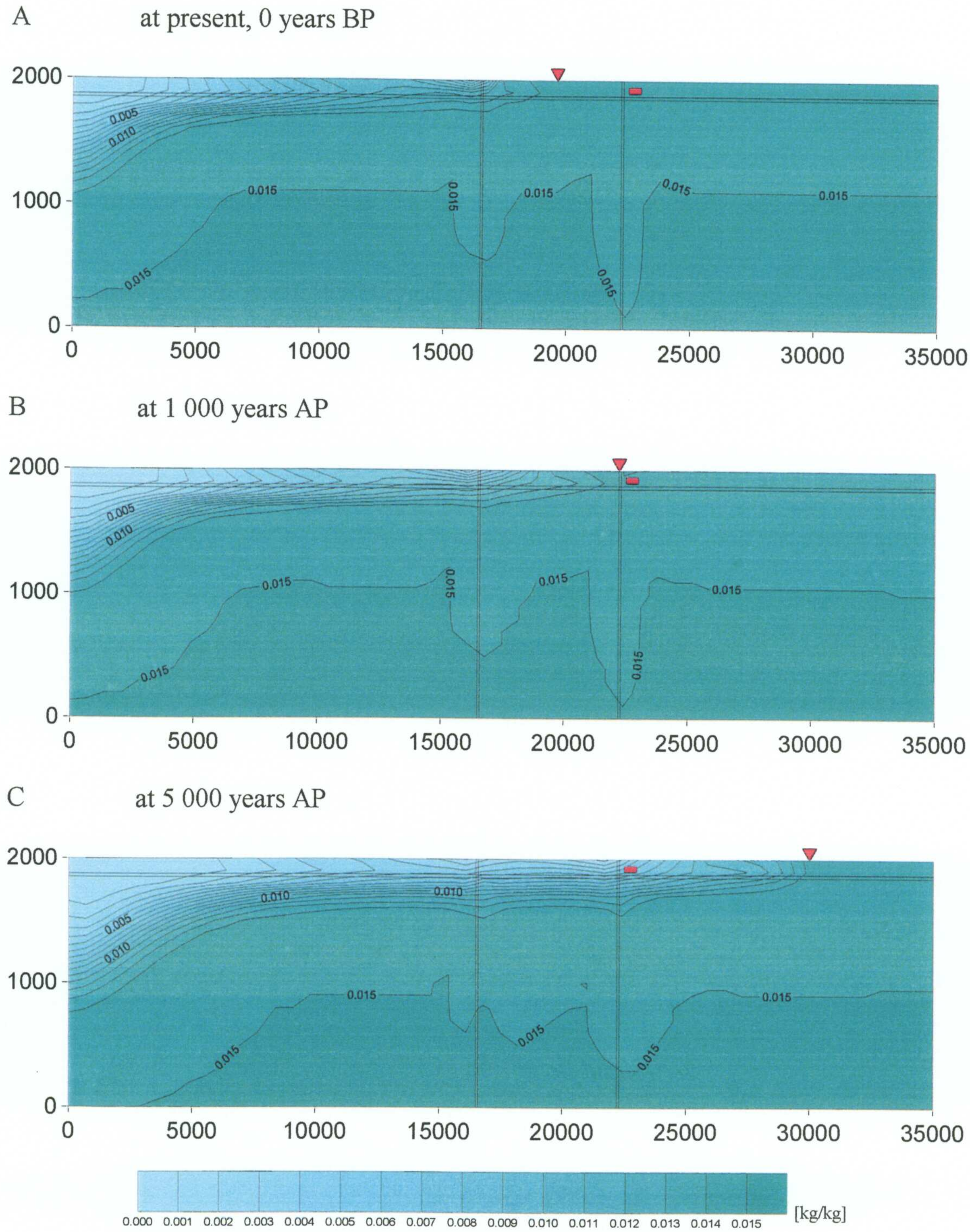

Figure 4-19. *Interplay between vertical and horizontal structures, for the case with variable-density. Once again it is shown that horizontal high permeable layers are important. The impact from the vertical zones is smaller in this case than it is for the case without the vertical zone, c.f. Figure 4-13. SFR is marked with a square and the shoreline with a triangle. The zone at 16 500 m corresponds to The Forsmark zone while the Singö zone is situated at 22 200 m. The horizontal zone, H2, is located at a depth of 125 m. Observe that the scale of the vertical axis is 5 times the horizontal*

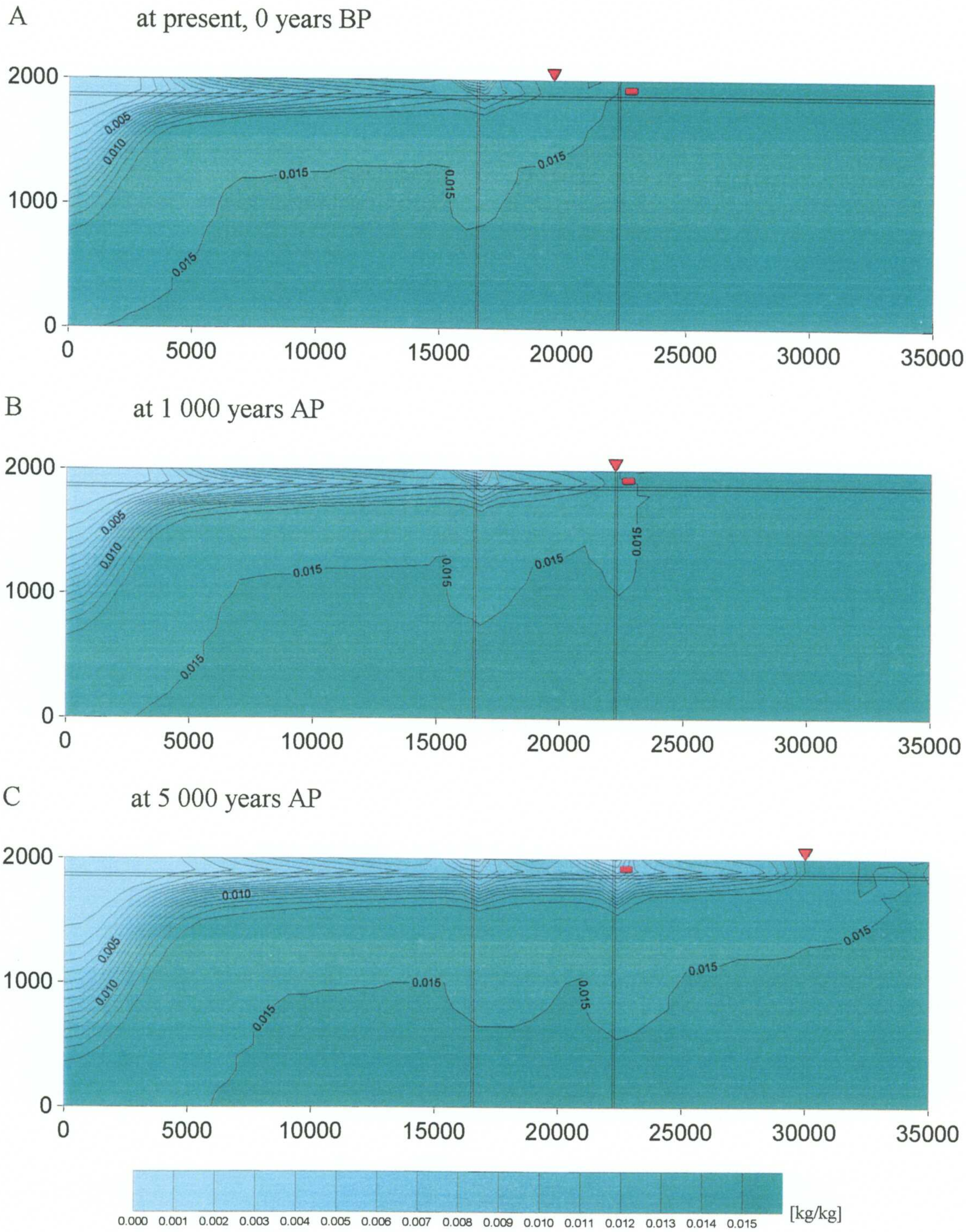

Figure 4-20. *Case with uniform-density and high permeable zones. A comparison with Figure 4-19 shows that the more complex the model is the less the spatial differences in salinity between the two approaches become. SFR is marked with a square and the shoreline with a triangle. The zone at 16 500 m corresponds to The Forsmark zone while the Singö zone is situated at 22 200 m. The zone H2 is located at a depth of 125 m. Observe that the scale of the vertical axis is 5 times the horizontal.*

4.8.2 Flow at the SFR

Some differences occur when high permeable vertical and horizontal structures are implemented into the model, c.f. Figure 4-21. As long as the SFR is under the Baltic sea the differences are small, but when the shoreline passes over the SFR, 1100-1200 years AP, the differences increase. The Darcy velocity is slightly larger for the uniform-density approach, and the direction is 20° upwards.

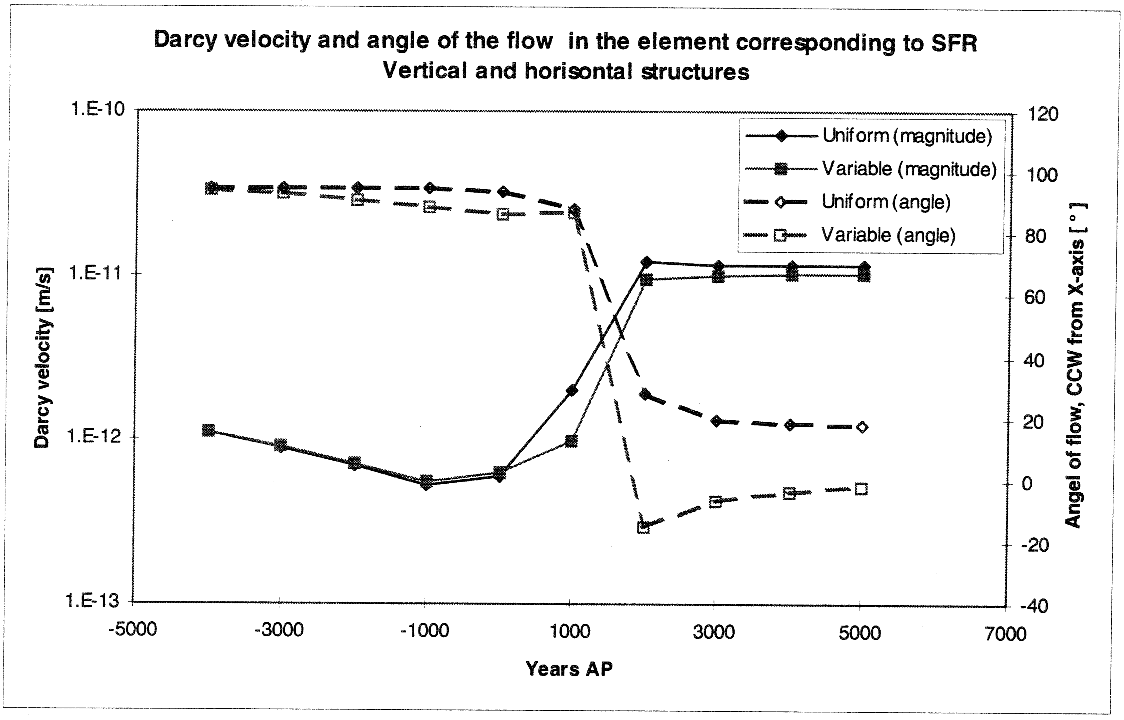

Figure 4-21. The magnitude and angle of the flow through the element that corresponds to the SFR for the case with high permeable vertical and horizontal structures.

The flow for the uniform-density approach is larger and directed more upwards than it is for the variable-density approach. This implies that the travel time for the water from the SFR to the surface will be shorter if a uniform-density approach is adopted.

4.9 Best estimate

As a comparison to the generic cases, studied in section 4.2 to 4.8, a "best estimate" model is made to investigate the distribution of salinity in a complex model.

This model uses knowledge of the properties of the structures and bedrock that are described in section 2.2. The porosity is 2‰ throughout the model domain. The evolution in salinity of the water in the Baltic Sea is set to have an initial value of 12‰ at 5 000 years BP that then decreases linearly to 5‰ today and remains constant for the next 5 000 years. The depth dependence of the hydraulic conductivity in the rock mass, and the properties for the zones are according to Axelsson and Hansen (1997). The extensions of the zones are that the Forsmark zone and the Singö zone are vertical and extend from the top to the bottom of the model. The zone H2 is sub-horizontal. The zone is terminated against the Forsmark zone and then extended to the sea bottom at 25 000 m.

4.9.1 Salinity in the modelled profile

As can be seen in Figure 4-22 and Figure 4-23 the spatial difference in salinity between the two density approaches is negligible. Most of the flow will occur in the upper, more permeable, part of the model. When the shore passes the Forsmark zone, at 16 500 m, the freshwater will flow downwards until the sub-horizontal zone, H2, intersects the Forsmark zone. Then the water will flow along this zone towards the Baltic Sea.

The most important conclusion is that the more complex the model is the less the spatial differences in salinity between variable-density and constant-density become.

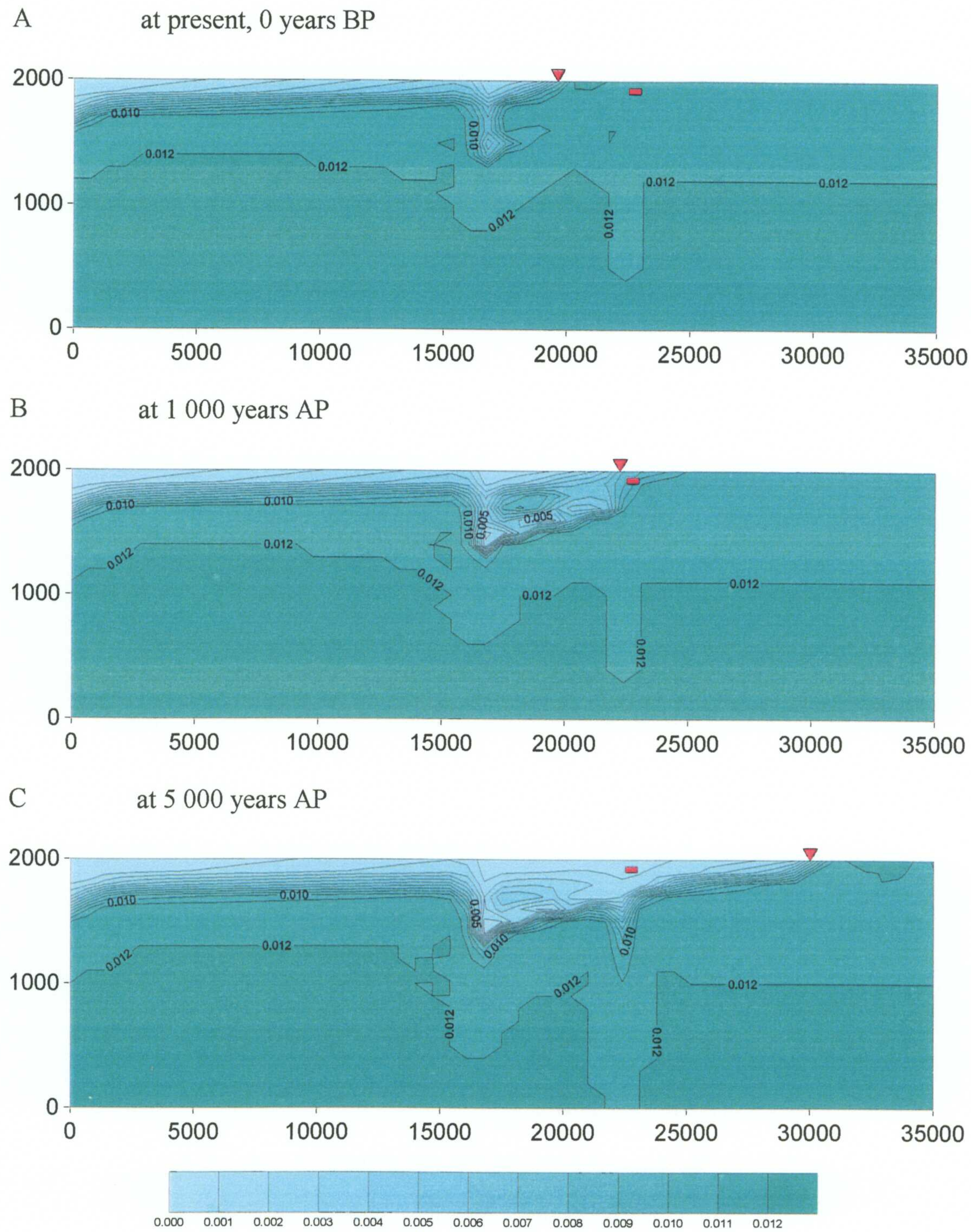

Figure 4-22. *Best estimate with variable-density. Most of the flow will occur in the upper, more permeable, part of the model domain or in the zones. SFR is marked with a square and the shoreline with a triangle. The zone at 16 500 m corresponds to The Forsmark zone while the Singö zone is situated at 22 200 m. The zone H2 is terminated against the Forsmark zone at a depth of 700 m and then extended to the sea bottom at 25 000 m. Observe that the scale of the vertical axis is 5 times the horizontal.*

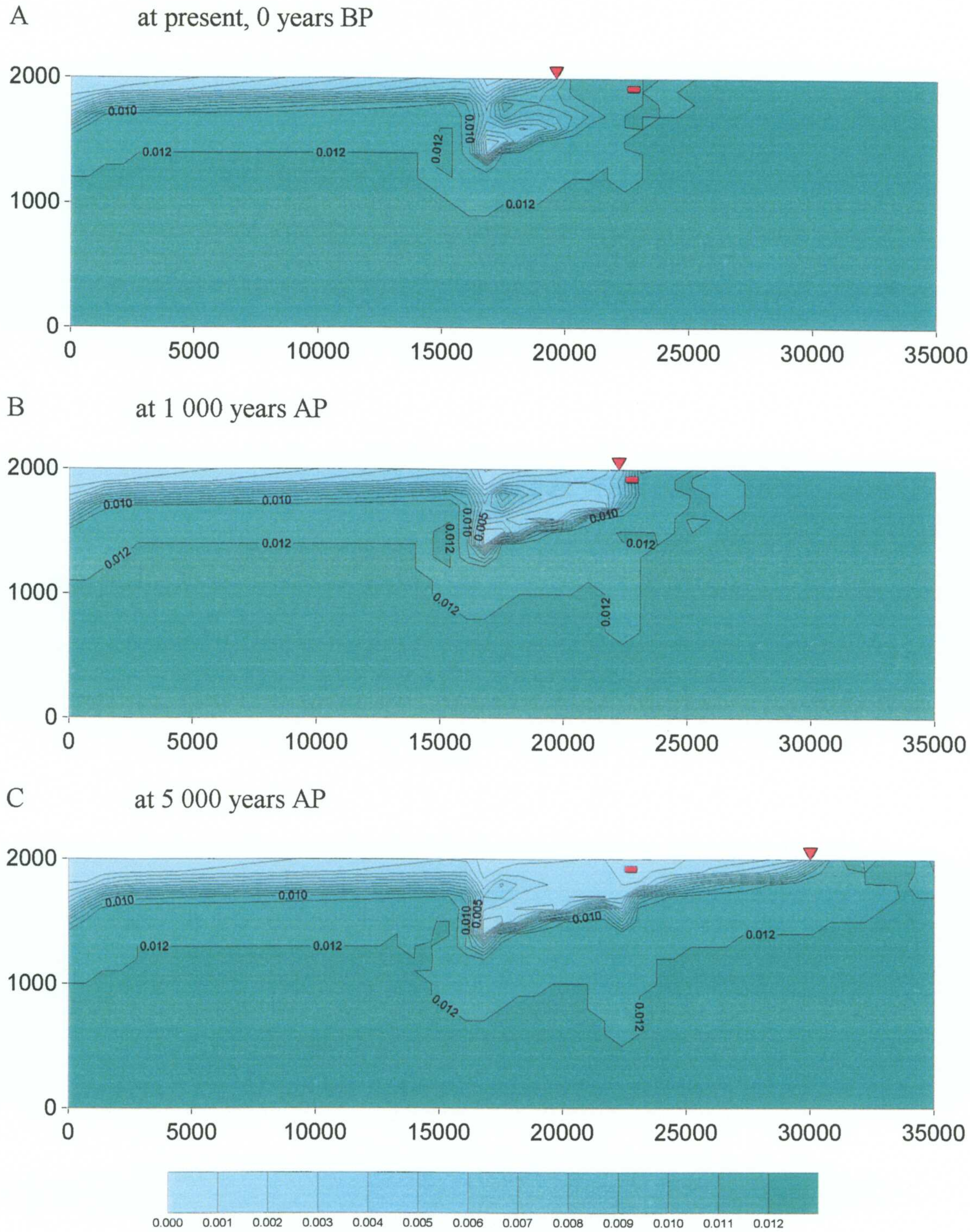

Figure 4-23. *Uniform-density in the best estimate case. A comparison with Figure 4-22 shows that the spatial difference in salinity between the approach with variable-density and with uniform-density is negligible when a complex modell is studied. The zone at 16 500 m corresponds to The Forsmark zone while the Singö zone is situated at 22 200 m. The zone H2 is terminated against the Forsmark zone at a depth of 700 m and then extended to the sea bottom at 25 000 m. Observe that the scale of the vertical axis is 5 times the horizontal*

4.9.2 Flow at the SFR

Some differences occur as long as the SFR is situated under the Baltic Sea. When the uniform-density approach is adopted the flow will be straight up the sea bottom, while it will be slightly tilted away from the coastline if the variable-density approach is adopted, see Figure 4-24. During a short period the direction of the flow is downwards towards the Singö zone when different density is assumed. After the shoreline has passed the flow is parallel to the surface for both approaches.

There is a small difference in the Darcy velocity as long as the SFR is under the seawater, but as soon as the shoreline has withdrawn the differences are negligible.

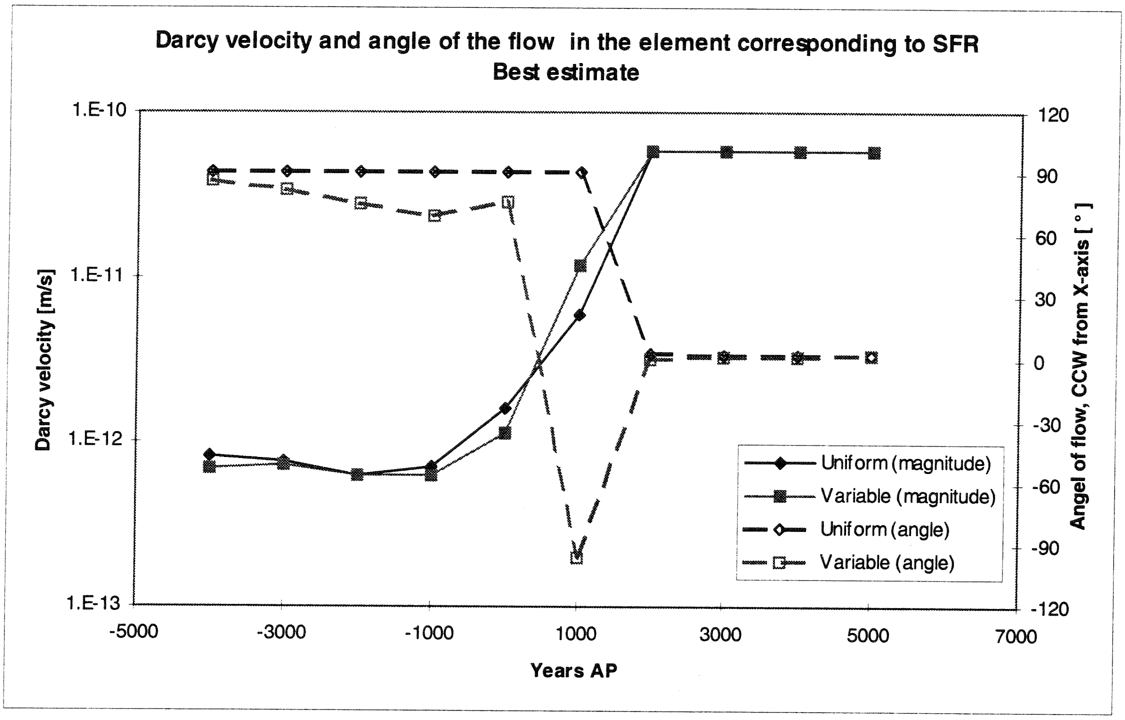

Figure 4-24. The magnitude and angle of the flow through the element that corresponds to the SFR for the best estimate case.

Conclusion from the best estimate model is that the differences in the flow are small when a complex model is studied, especially after that the shoreline has passed over the SFR.

5 Conclusions

This report investigates whether variable-density groundwater flow at the SFR can be treated as uniform-density flow where salinity is modelled as a tracer. Secondly, the work also addresses the sensitivity of the various model parameters, such as permeability, porosity, structures and salinity in seawater, on the model results. The conclusions from this modelling study are:

- Fresh water will float on top of saline water if the hydrogeologic system is modelled as a variable-density system.
- The considered progress in salinity of the seawater does not have an impact on the results as compared to the reference case.
- High permeable layers and structures have a large impact on the results since the flow will follow the path with the highest permeability.
- The porosity has a large impact on the results since higher porosity means that the transport time increases and that more saline water has to be flushed out.
- There are only small differences in the Darcy velocity between the variable-density and the uniform-density approach, especially after that the shoreline has passed the SFR.
- There are some differences in the direction of the flow. In most of these cases the difference will underestimate the transport time if a uniform-density approach is adopted.
- As the model becomes more complex (i.e., incorporating parameter heterogeneity, structures etc.) the spatial differences in salinity and the difference in flow through the SFR, between variable-density and uniform-density flow, become less significant.
- Differences between modelling groundwater as a variable-density flow or a uniform-density flow with salt as a tracer at the SFR are negligible.

REFERENCES

Ahlbom, K., J.-E. Andersson, P. Andersson, T. Ittner, C. Ljunggren and S. Tirén (1992) Finnsjön study site. Scope of activities and main results, SKB TR 92-33, Swedish Nuclear fuel and Waste Management Corporation, Stockholm.

Axelsson, C.-L., L. Carlsson and T. Svensson (1983) SFR-Bedömningar av utströmningsområden för grundvatten, SGAG and SGU, Göteborg and Uppsala.

Axelsson, C.-L. (1986) Modeling of groundwater flow with salt-water interface at the final repository for reactor waste (SFR), Uppsala Geosystem AB, under SSI contract no. SSI P 311.85

Axelsson, C.-L. and L. Hansen (1997) Update of structural models at SFR nuclear waste repository, Forsmark, Sweden, SKB R-98-05, Swedish Nuclear fuel and Waste Management Corporation, Stockholm.

Carlsson, A. and T. Olsson (1981) Hydraulic properties of a fractured granitic rock mass at Forsmark, Sweden, SGU C 783, Uppsala.

Carlsson, L., A. Winberg and J. Arnefors (1986) Hydraulic modeling of the final repository for reactor waste (SFR). Compilation and Conceptualization of Available Geological and Hydrogeological Data, SKB PR SFR 86-03, Swedish Nuclear fuel and Waste Management Corporation, Stockholm.

Carlsson, L., B. Grundfeldt and A. Winberg (1987) Hydraulic modelling of the final repository for reactor waste (SFR). Evaluation of the groundwater flow situation at SFR, SKB PR SFR 86-07, Swedish Nuclear fuel and Waste Management Corporation, Stockholm.

Follin, S. (1995) Geohydrological simulation of a deep coastal repository, SKB TR 95-33, Swedish Nuclear fuel and Waste Management Corporation, Stockholm.

Follin, S., M. Årebäck, G. Jacks (1996) Förstudie Östhammar, Grundvattnets rörelse, kemi och långsiktiga förändringar, SKB PR D-96-017, Swedish Nuclear fuel and Waste Management Corporation, Stockholm.

Kautsky, U. (1998) Variatoner i biosfären från senaste istiden till nästa istid med speciell referens till Äspö, PM 1998-02-10, Swedish Nuclear fuel and Waste Management Corporation, Stockholm.

Marine Ecosystem Modeling Group (1996), http://data.ecology.su.se/baltic96/, 20 Feb 1998, Department of Systems Ecology, Stockholm University, Sweden

Påsse, T. (1996) A mathematical model of the shore level displacement in Fennoscandia, SKB TR 96-24, Swedish Nuclear fuel and Waste Management Corporation, Stockholm.

SKB, (1993) Slutförvar för radioaktivt driftavfall - SFR1. Slutlig säkerhetsrapport. Reviderad utgåva - Maj 1993, Swedish Nuclear fuel and Waste Management Corporation, Stockholm.

SKB, (1998) Appendix 4C in Project SAFE, Update of the SFR-1 safety assessment phase 1, SKB Report R 98-44, Swedish Nuclear fuel and Waste Management Corporation, Stockholm.

Walker, D., Rhén, I., Gurban, I., SR 97, (1997) Summary of hydrogeologic conditions at Aberg, Beberg and Ceberg, SKB TR 97-06, Swedish Nuclear fuel and Waste Management Corporation, Stockholm.

VBB (1973) Angående grundförhållandena för hamn och farledsränna vid Forsmark kraftstation, VBB Teknisk rapport, Stockholm

Westman P., Saliniteten i Östersjön sedan senaste istiden, 1997, Kvartärgeologiska Instutitionen Stockholms universitet.

Voss, C. I. (1984) SUTRA - A finite-element simulation model for saturated-unsaturated, fluid-density-dependent ground-water flow with energy transport or chemically-reactive single-species solute transport, U.S. Geological Survey Water-Resources Investigations Report 84-4369, U.S. Geological Survey, Reston, VA.

Voss. C. I. and J. Andersson (1993) Regional flow in the Baltic shield during holocene coastal regression, Ground Water, vol 31 no 6 pp 989-1006.

A mathematical expression for converting conventional ^{14}C-dates to calendar dates is derived in Påsse (1996). The formula is:

$$T = 59.6-206.9\cdot ATAN((4000-1.095\cdot T_{con})/800)+63.66\cdot ATAN((7200-1.095\cdot T_{con})/100)+95.5\cdot ATAN((750-1.095\cdot T_{con})/200)+1.095\cdot T_{con}$$

Where:

T = Calendar date

T_{con} = Conventional radiocarbon date

In figure A-1 calendar years are plotted against ^{14}C years

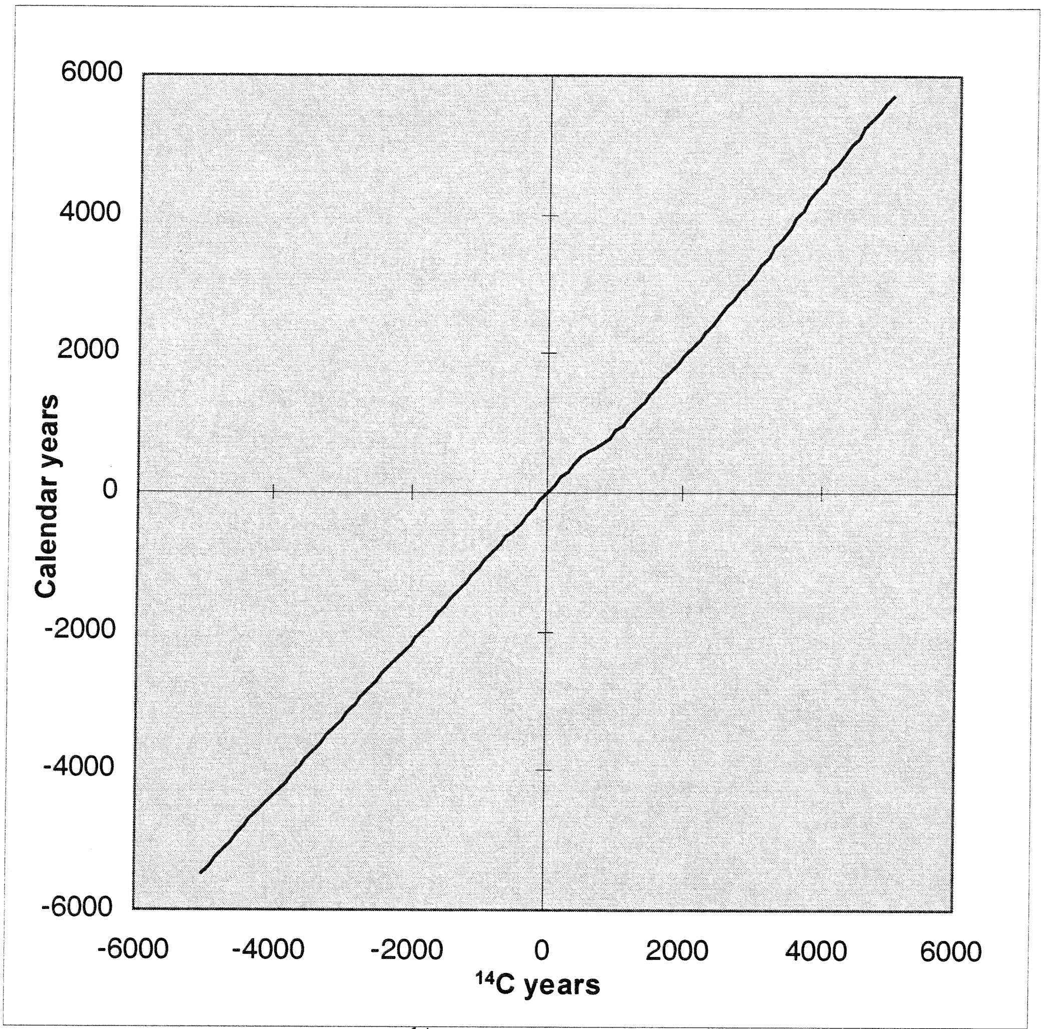

Figure A-1. *Calendar years versus ^{14}C years.*